The yeast homologue of the microtubule-associated protein Lis1 interacts with the sumoylation machinery and a SUMO-targeted ubiquitin ligase

Annabel Alonso[a], Sonia D'Silva[b], Maliha Rahman[a], Pam B. Meluh[c], Jacob Keeling[a], Nida Meednu[b], Harold J. Hoops[d], and Rita K. Miller[a]
[a]Department of Biochemistry and Molecular Biology, Oklahoma State University, Stillwater, OK 74078; [b]Department of Biology, University of Rochester, Rochester, NY 14627; [c]Department of Molecular Biology and Genetics, Johns Hopkins University School of Medicine, Baltimore, MD 21205; [d]Department of Biology, State University of New York, Geneseo, NY 14454

ABSTRACT Microtubules and microtubule-associated proteins are fundamental for multiple cellular processes, including mitosis and intracellular motility, but the factors that control microtubule-associated proteins (MAPs) are poorly understood. Here we show that two MAPs—the CLIP-170 homologue Bik1p and the Lis1 homologue Pac1p—interact with several proteins in the sumoylation pathway. Bik1p and Pac1p interact with Smt3p, the yeast SUMO; Ubc9p, an E2; and Nfi1p, an E3. Bik1p interacts directly with SUMO in vitro, and overexpression of Smt3p and Bik1p results in its in vivo sumoylation. Modified Pac1p is observed when the SUMO protease Ulp1p is inactivated. Both ubiquitin and Smt3p copurify with Pac1p. In contrast to ubiquitination, sumoylation does not directly tag the substrate for degradation. However, SUMO-targeted ubiquitin ligases (STUbLs) can recognize a sumoylated substrate and promote its degradation via ubiquitination and the proteasome. Both Pac1p and Bik1p interact with the STUbL Nis1p-Ris1p and the protease Wss1p. Strains deleted for *RIS1* or *WSS1* accumulate Pac1p conjugates. This suggests a novel model in which the abundance of these MAPs may be regulated via STUbLs. Pac1p modification is also altered by Kar9p and the dynein regulator She1p. This work has implications for the regulation of dynein's interaction with various cargoes, including its off-loading to the cortex.

INTRODUCTION

Microtubules are critical for a number of basic cellular processes. They are vital to the operation of the mitotic spindle. They can act as ropes that pull on kinetochores to separate the attached chromosomes. Microtubules also function as tracks that guide the transport of various cargoes to distinct destinations within the cell. Many aspects of microtubule function are regulated by distinct classes of microtubule-binding proteins.

In the yeast *Saccharomyces cerevisiae*, microtubules are critical for positioning the mitotic spindle, a process governed by two genetic systems termed the Kar9 pathway and the dynein pathway. The Kar9 pathway orients cytoplasmic microtubules into the bud, and the dynein pathway pulls on the cytoplasmic microtubules to position the spindle across the bud neck with the onset of anaphase (Kahana *et al.*, 1995; Yeh *et al.*, 1995; Carminati and Stearns, 1997; Miller *et al.*, 1998). In the dynein pathway, both Bik1p and Pac1p help localize dynein to the plus end of the microtubule before it is "off-loaded" to the cortex (Sheeman *et al.*, 2003; Lee *et al.*, 2005; Caudron *et al.*, 2008; Markus *et al.*, 2011). The microtubule-binding protein Bik1p is a member of the CLIP-170 family, and Pac1p is a member of the Lis1 family.

Bik1p is a multifunctional protein. Bik1p is found on both nuclear and cytoplasmic microtubules (Berlin *et al.*, 1990; Sheeman *et al.*, 2003; Miller *et al.*, 2006). It stabilizes microtubules, and in its absence, microtubules are very short (Berlin *et al.*, 1990; Blake-Hodek *et al.*, 2010). It also acts to tether microtubules to the cell cortex in mating cells (Molk *et al.*, 2006). Whereas the mammalian CLIP-170 binds growing microtubules only, the yeast Bik1p tracks both the growing and shrinking ends of microtubules (Carvalho *et al.*, 2004). In the nucleus, Bik1p is also part of the kinetochore, and its activity there has been linked to preanaphase kinetochore separation in polyploid strains (He *et al.*, 2001; Lin *et al.*, 2001). However, its precise role at kinetochores remains unclear (Westermann *et al.*, 2007). Bik1p localization at the plus end of cytoplasmic microtubules is mediated by the kinesin motor, Kip2p, which carries it to the plus end (Carvalho *et al.*, 2004; Caudron *et al.*, 2008).

Bik1p and Pac1p are each structurally similar to their mammalian counterparts. Bik1p is composed of an amino-terminal head domain, a central coiled-coil domain, and a carboxy-terminal tail (Miller *et al.*, 2006). In its head domain, Bik1p has one CAP-Gly domain for microtubule binding, whereas CLIP-170 has two. This is followed by a serine-rich domain, which may be used in phosphoregulation (Miller *et al.*, 2006). A 40–amino acid region at the carboxy-terminus termed the cargo-binding domain is required for interaction with dynein and Pac1p (Lin *et al.*, 2001; Sheeman *et al.*, 2003; Li *et al.*, 2005). The structure of Pac1p includes a short coiled-coil domain and a highly conserved WD40 repeat domain. Neither of the two domains alone is sufficient for microtubule binding or plus-end tracking in vivo (Markus *et al.*, 2011).

Mutations in Lis1 cause lissencephaly, a devastating disease of abnormal brain development resulting from incomplete neuronal migration (Reiner *et al.*, 2006). Lis1 has a number of activities associated with microtubules. Lis1 function is closely linked to dynein, a minus end–directed motor protein that regulates a number of different movements within the cell, including vesicle transport, mitosis, cell migration, nuclear migration, and spindle orientation (Faulkner *et al.*, 2000; Dujardin *et al.*, 2003; Shu *et al.*, 2004; Tanaka *et al.*, 2004; Tsai *et al.*, 2005, 2007, 2010; Lam *et al.*, 2010; Zhang *et al.*, 2010). As an adaptor to dynein, Lis1 modulates a subset of dynein functions (Faulkner *et al.*, 2000). Lis1 also interacts with the motor domain of dynein and affects its motor activity (McKenney *et al.*, 2010; Torisawa *et al.*, 2011; Huang *et al.*, 2012). In doing so, it increases the time that dynein interacts with the microtubule, making dynein more persistent in generating force for transport of heavy loads (McKenney *et al.*, 2010, 2011). Furthermore, Lis1 coordinates the activity of plus end–directed motors with minus end–directed motors (Yi *et al.*, 2011). Lis1 can also affect microtubule assembly, both positively or negatively (Sapir *et al.*, 1997; Han *et al.*, 2001). In the upper layers of the epithelium, Lis1 is important for the organization of cortical microtubules and the stability of desmosomes (Sumigray *et al.*, 2011). In yeast, Pac1p functions in the dynein pathway by working with Bik1p to recruit dynein to the plus end of the microtubule (Lee *et al.*, 2003; Sheeman *et al.*, 2003; Li *et al.*, 2005; Markus *et al.*, 2011). Although much is known about the various activities of Lis1, little is known about the regulation of Lis1 and/or Pac1p in each of these different contexts.

Proteins in both the Kar9p and dynein pathways have been shown to be regulated by phosphorylation (Choi *et al.*, 2000, 2002; Liakopoulos *et al.*, 2003; Maekawa and Schiebel, 2004; Moore *et al.*, 2006, 2008). However, little is known about how other protein modifications regulate spindle positioning.

Sumoylation is a small ubiquitin-like modification that regulates many divergent cellular processes and is key to several diseases

(reviewed in Dasso, 2008; Gareau and Lima, 2010; Sarge and Park-Sarge, 2011; Praefcke *et al.*, 2012). In yeast, the single gene for SUMO is *SMT3*. SUMO conjugation onto target lysines occurs through a terminal glycine residue, which becomes exposed by the action of the Ulp1p protease, which removes the last three amino acids of SUMO. A cascade of enzymes analogous to, yet distinct from, ubiquitination is responsible for SUMO conjugation to its substrates. The E1 dimer Aos1p–Uba2p activates Smt3p in an ATP-dependent step. The E2-conjugating enzyme is Ubc9p. Four E3 ligases are known in yeast that also confer substrate specificity. These are Nfi1/Siz1p, Siz2p, Nse2p, and Mss21p (Johnson and Gupta, 2001; Reindle *et al.*, 2006; Duan *et al.*, 2011; Heideker *et al.*, 2011; Stephan *et al.*, 2011).

Removal of SUMO from targets is a dynamic process, and SUMO deconjugation is important for cellular health (Bekes *et al.*, 2011). Three proteases remove SUMO from its targets in yeast. These are Ulp1p, Ulp2p, and Wss1p (Mukhopadhyay and Dasso, 2007; Kolli *et al.*, 2010; Mullen *et al.*, 2010). Ulp1p is an essential protease required for cell cycle progression that localizes to the nuclear envelope and septin ring (Li and Hochstrasser, 1999; Elmore *et al.*, 2011). The Ulp2p has chain-editing activity and can cleave SUMO chains, acting to shorten their length (Bylebyl *et al.*, 2003; Mukhopadhyay *et al.*, 2007; Yeh, 2009). The protease Wss1p displays SUMO-isopeptidase activity and is reported to be associated with the proteasome (Mullen *et al.*, 2010). Ulp1p and Ulp2p are SUMO specific, whereas Wss1p may remove both ubiquitin and SUMO (Mullen *et al.*, 2010; Su and Hochstrasser, 2010).

In 2007, a new mode of cross-talk was identified between the ubiquitination and sumoylation systems (Sun *et al.*, 2007; Uzunova *et al.*, 2007; Xie *et al.*, 2007). SUMO targeted ubiquitin ligases (STUbLs) are ubiquitin ligases that recognize a sumoylated protein and polyubiquitinate it, sending the target to the proteasome for degradation. How STUbLs interact with microtubule-binding proteins is not known.

Recent work suggests that sumoylation regulates the Kar9p spindle-positioning pathway by modifying the Kar9 protein (Leisner *et al.*, 2008; Meednu *et al.*, 2008). Defects in sumoylation alter the localization of Kar9p to both spindle poles rather than just the pole destined for the bud (Leisner *et al.*, 2008; Meednu *et al.*, 2008). In the present study, we show that two proteins from the dynein pathway, Bik1p and Pac1p, interact with SUMO and several proteins from the SUMO conjugating and processing system. We also show that the SUMO protease Ulp1p controls the amount of shifted Pac1p. Both Bik1p and Pac1p also interact with the STUbL enzyme dimer Nis1p–Ris1p. Taken together, our findings suggest that these microtubule-associated proteins may be regulated by the SUMO signal transduction system. This could have implications for the regulation of CLIP-170 and Lis1 family members in other systems.

RESULTS
Both Bik1p and Pac1p interact with the yeast SUMO Smt3p
Bik1p interacts physically with Kar9p, and Kar9p is sumoylated (Moore *et al.*, 2006; Leisner *et al.*, 2008; Meednu *et al.*, 2008). We therefore investigated whether proteins in the dynein pathway might also be regulated by sumoylation. We tested for an interaction between Smt3p and two proteins that function in the dynein pathway, Bik1p and Pac1p, by two-hybrid analysis. As shown in Figure 1, both *BIK1* and *PAC1* interacted with *SMT3*. *BIK1* did not interact with ubiquitin encoded by *UBI4* or the small ubiquitin-related protein encoded by *URM1*. In contrast, *PAC1* also displayed a slight but consistently detectable interaction with ubiquitin. As previously reported, the kinesin motor protein encoded by *KIP2*
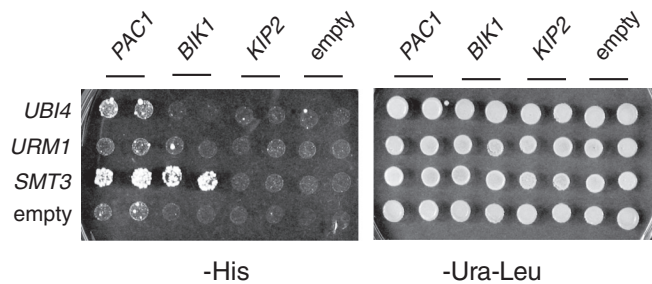
FIGURE 1: *BIK1* and *PAC1* interact with SUMO/*SMT3* by two-hybrid analysis. Yeast ubiquitin is encoded by *UBI4*, and the ubiquitin-related modifier is encoded by *URM1*. Diploid two-hybrid reporter strains were generated by crossing yRM1757/PJ65-4A containing *PAC1*-BD (pRM3604), *BIK1*-BD (pRM4924), *KIP2*-DB (pRM3595), or empty-BD (pRM1154) with yRM1756/PJ69-4A containing activation domain (AD)-*UBI4* (pRM5880), AD-*URM1* (pRM5829), AD-*SMT3* (pRM4920), or empty AD (pRM1151). Diploids were selected on SC–ura–leu and tested for interaction by growth on SC–his at 30°C for 2–3 d. Two independent diploid colonies were tested. Although *UBI4*, *URM1*, and *SMT3* are members of the same protein superfamily, only *SMT3* interacted strongly with both *BIK1* and *PAC1*.

did not interact with *SMT3* (Meednu *et al.*, 2008). Thus two-hybrid analysis of three members of the ubiquitin superfamily suggests that Bik1p and Pac1p interact strongly with Smt3p.

Bik1p and Pac1p interact with Smt3p-GG but not with Smt3p-GA

The protease Ulp1p is responsible for removing the carboxyl three amino acids from full-length Smt3p. This exposes a glycine at position 98 for conjugation to substrates. The absence of this terminal glycine precludes conjugation to target proteins (Johnson and Blobel, 1997). We therefore tested whether two mutations would abrogate the interaction. The first mutation deletes the last three amino acids (ATY), exposing the terminal diglycine motif (*SMT3*-GG). The second mutation replaces the terminal glycine with alanine (*SMT3*-GA), preventing conjugation. As shown in Figure 2A, full-length *SMT3* and the truncated form of *SMT3*, *SMT3*-GG, interacted with both *BIK1* and *PAC1*, but the *SMT3*-GA form did not. Previous work demonstrated that the *SMT3*-GA construct was expressed (Meednu *et al.*, 2008). This suggests the possibility that conjugation mediates the two-hybrid interactions of Bik1p and/or Pac1p with Smt3p.

Bik1p and Pac1p interact with other enzymes in the sumoylation pathway

Several enzymes in the sumoylation pathway facilitate the transfer of SUMO to target proteins. Kar9p was previously shown to interact with several of these by two-hybrid analysis (Meednu *et al.*, 2008). Both *BIK1* and *PAC1* interacted with *UBC9* encoding the E2 enzyme and *NFI1/SIZ2* encoding an E3 enzyme (Figure 2B). Thus two proteins from the dynein pathway interact with multiple enzymes required for sumoylation.

Bridging

A yeast two-hybrid interaction can be explained most simply by a direct binding of the bait and prey proteins. However, if a third protein binds between the bait and prey, it might activate transcription of the reporter gene and falsely suggest a direct interaction. Bik1p interacts with two other spindle-positioning proteins, Kar9p and Bim1p (Schwartz *et al.*, 1997; Moore *et al.*, 2006; Wolyniak *et al.*,
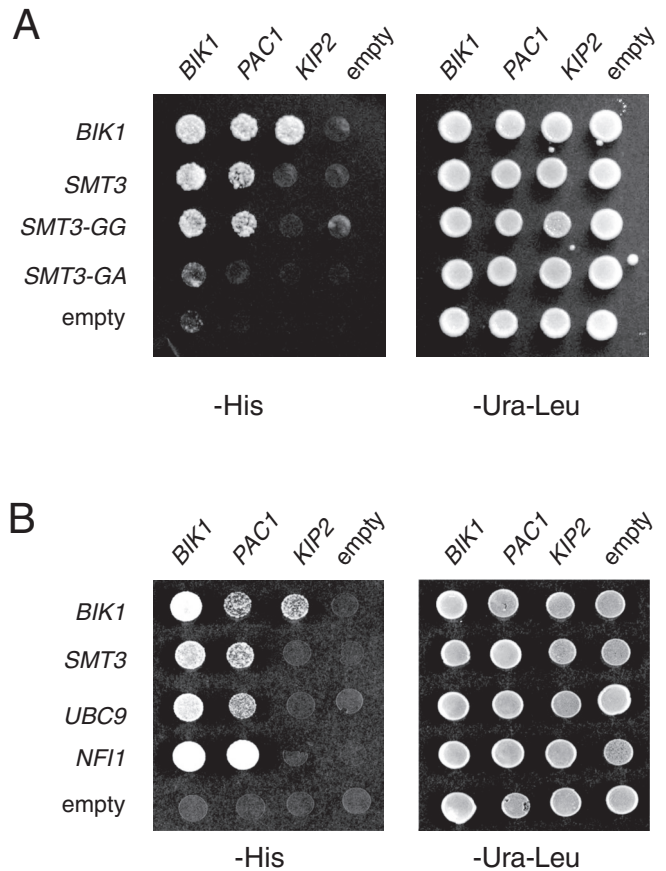
A

B

FIGURE 2: *PAC1* and *BIK1* interact with multiple genes in the sumoylation pathway by two-hybrid analysis. Two-hybrid reporter strains (yRM1757/PJ69-4A) containing *BIK1*-BD (pRM4924), *PAC1*-BD (pRM3604), *KIP2*-BD (pRM3595), or empty BD (pRM1154) were mated to reporter strains (yRM1756/ PJ69-4α) containing AD-*BIK1* (pRM2627), AD-*SMT3* (pRM4920), AD-*SMT3*-GG (pRM4382), AD-*SMT3*-GA (pRM4383), AD-*UBC9* (pRM4495), AD-*NFI1* (pRM4496), or empty AD (pRM4380) plasmids. Diploids were selected on media lacking uracil and leucine (–ura –leu) and assayed for interactions on media lacking histidine (–his). AD-*SMT3* encodes full-length *SMT3*. In the AD-*SMT3*-GG construct, the last three amino acids have been truncated, exposing glycine 98 as the terminal amino acid. In the AD-*SMT3*-GA construct, glycine 98 has been replaced by an alanine residue. The kinesin encoded by *KIP2* transports Bik1p along microtubules (Carvalho *et al.*, 2004) and serves as an extra negative control here. The *KIP2*-BD construct is functional, as shown by the interaction between *BIK1* and *KIP2*.

2006), both of which also interact with Smt3p (Meednu *et al.*, 2008). To investigate whether either Kar9p or Bim1p could serve as a bridge in the two-hybrid interaction between Bik1p and Smt3p, we tested the two-hybrid interaction in a reporter strain deleted for either of these genes. As shown in Figure 3, A and B, neither *KAR9* nor *BIM1* is required for the interaction. We also tested whether *PAC1* was required for the interaction of Kar9p with the SUMO pathway. As shown in Figure 3C, no difference was observed for the interaction in the *pac1Δ* and wild-type strains, suggesting that the interaction of Kar9p with sumoylation proteins does not require Pac1p.

Because Bik1p also interacts with Pac1p (Sheeman *et al.*, 2003), we next considered the simple bridging model in which Pac1p might bridge the two-hybrid interaction between Bik1p and Smt3p or vice versa. To test this, we deleted either *BIK1* or *PAC1* from the
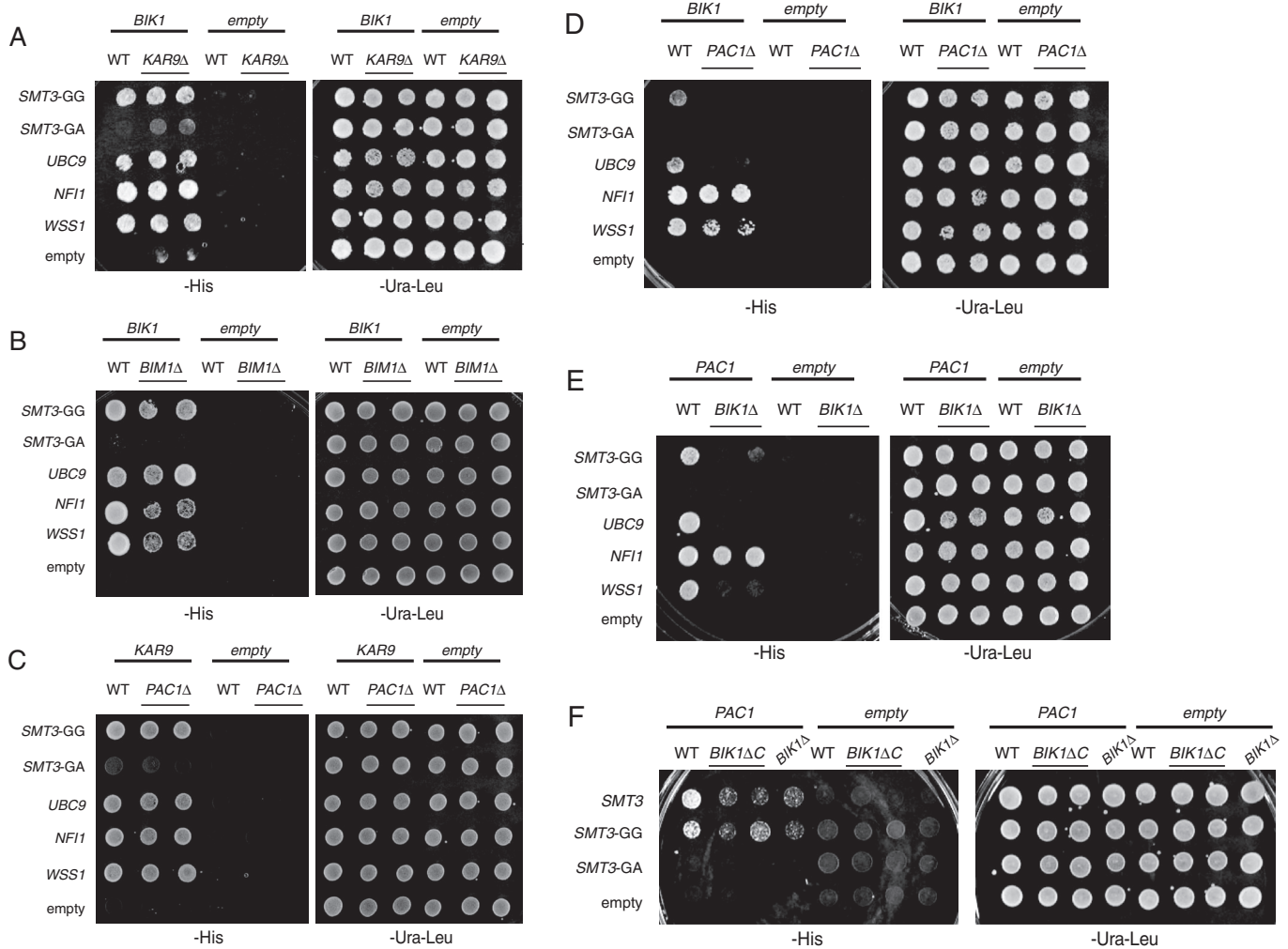
FIGURE 3: The interaction of *PAC1* with *SMT3* is enhanced by *BIK1*. (A) The interaction of *BIK1* with genes in the sumoylation pathway does not require *KAR9*. Either wild-type (yRM1757) or two-hybrid reporter strains disrupted for *KAR9* (*kar9Δ*, yRM6172) were transformed with the following constructs: *KAR9*-BD, empty BD, AD-*SMT3*, AD-*SMT3*-GG, AD-*SMT3*-GA, AD-*UBC9*, AD-*NFI*, AD-*WSS1*, or empty AD. For this assay, haploid reporter strains were used. The interactions were assayed on media lacking histidine (–his). Two colonies of *BIK1*-BD and empty BD were tested in the *kar9Δ* strain. One colony of the wild-type strain is shown for comparison. (B) The interaction of *BIK1* with genes in the sumoylation pathway does not require *BIM1*. Either the wild-type (yRM1757) or a two-hybrid reporter strain deleted for *BIM1* (yRM2057) was transformed with the plasmids described A. Two colonies of *BIK1*-BD and empty BD in *bim1Δ* were tested. (C) The *KAR9-SMT3* interaction does not require *PAC1*. The interactions of *KAR9* (pRM1493) were analyzed in either a wild-type (yRM1757) or a two-hybrid reporter strain deleted for *PAC1* (yRM6249), using the constructs and conditions described. (D) *BIK1* requires *PAC1* for interaction with *SMT3*. Either wild-type (yRM1757) or a two-hybrid reporter strain deleted for *PAC1* (yRM6249) was transformed with the indicated constructs. (E) *PAC1* requires *BIK1* for interactions with some sumoylation genes. AD-*SMT3*, AD-*SMT3*-GG, AD-*SMT3*-GA, AD-*UBC9*, AD-*NFI*, AD-*WSS1*, or empty AD was transformed into the two-hybrid reporter strain containing either *PAC1*-BD (pRM3604) or empty BD (pRM1154). Two two-hybrid reporter strains were used, wild-type strain (yRM1757) and a strain deleted for *BIK1* (yRM2258). The transformants possessing both BD and AD constructs were selected on the media lacking uracil and leucine. To test for the interaction, the transformants from both wild-type and *bik1Δ* strains were transferred to a plate with media lacking histidine (–his). One colony of the wild-type and two colonies of *bik1Δ* strain were analyzed. (F) The *PAC1-SMT3* interaction requires the cargo-binding domain of *BIK1*. Two-hybrid analysis was carried out in a haploid wild-type reporter strain (yRM1757) and an isogenic reporter strain deleted for the carboxy-terminal 40 amino acids of Bik1p, *bik1ΔC40* (yRM6444). The cargo-binding domain is required for the Bik1p–Pac1p interaction (Sheeman *et al.*, 2003). The indicated BD fusion and AD fusions were used. Two independent colonies carrying the *bik1ΔC40* mutation are shown, as well as one colony each for the wild-type and *bik1Δ* deletion strains. The presence of the truncated Bik1p in the reporter strain was confirmed by Western blotting (unpublished data).

two-hybrid reporter strain. To our surprise, the deletion of either gene resulted in the loss of Smt3p's interaction with the reciprocal protein (Figure 3, D and E). This result is not consistent with a simple bridging model in which Bik1p bridges Pac1p and Smt3p or Pac1p bridges Bik1p and Smt3p. Instead, we speculate that the cointeraction of Bik1p with Pac1p promotes a synergistic interaction with

Smt3p. Work from the Pellman lab showed that the cargo-binding domain of Bik1p is required for its two-hybrid interaction with Pac1p (Sheeman *et al.*, 2003), suggesting that this domain may mediate the Bik1p–Pac1p interaction. To gain insight into the Pac1p– Smt3p interaction, we deleted the cargo-binding domain of Bik1p from the two-hybrid reporter strain. The absence of the cargo-binding domain greatly diminished the interaction between *PAC1* and *SMT3* (Figure 3F). This finding is consistent with Smt3p interacting with a complex of Bik1p–Pac1p. Further testing of this model will require the identification of a *PAC1* allele that does not interact with Bik1p.

Bik1p can be sumoylated in vitro and in vivo

To determine whether Bik1p is a target for sumoylation, we analyzed Bik1p in an in vitro sumoylation assay using recombinant Smt3p, Ubc9p, and Uba2p/Aos1p purified from bacteria. Bik1p isoforms were separated on SDS–PAGE and analyzed by Western blotting. Two, and possibly three, higher–molecular weight forms of Bik1p were observed in the test lane (Figure 4A, lane 1) but not in the control reactions, each lacking the respective component of the assay (lanes 2–6). These results are consistent with two possibilities. Bik1p sumoylation may occur on at least two sites or polysumoylation might occur by the formation of SUMO chains.

Sumoylation frequently occurs on a lysine residue contained within the consensus motif, $\Psi KxD/E$, where Ψ is a hydrophobic amino acid, x is any amino acid, and D/E is an aspartic or glutamic acid. Bik1p contains one $\Psi KxD/E$ consensus sequence, WKPD at K180, and two examples of a less well-conserved KxD/E motif, GKND at K46 and KKLEE at K373 and K374. Mutation of the four lysines to arginine within these three locations, as well as a mutation in an additional lysine at position K251, did not alter the shift seen in vitro (unpublished data). This indicates that nonstandard sites may be used in the sumoylation of Bik1p.

Next we investigated whether Bik1p is sumoylated in the cell. Bik1p-hexahistidine (his6) was isolated from cells either overexpressing Smt3p or containing an empty vector. Analysis by immunoblotting revealed a shifted form of Bik1p that was present only when Smt3p was overexpressed (Figure 4B, panel 1, lanes 1 and 3). This shifted band corresponded exactly to a band revealed in an identical blot electrophoresed simultaneously and probed with polyclonal Smt3p or anti-hemagglutinin (HA). This suggests that overexpression of Smt3p results in Bik1p sumoylation.

Pac1p, but not Bik1p, is shifted by inhibition of the Ulp1p protease

Ulp1p is a SUMO protease that cleaves SUMO from sumoylated targets. Inhibition of Ulp1p is predicted to increase the sumoylation levels of Ulp1p substrates (Li and Hochstrasser, 1999, 2000). To test this idea for Bik1p, we examined the levels of shifted Bik1p in *ulp1*-ts at the nonpermissive temperature of 37°C. However, despite numerous attempts using a variety of different conditions, we could not detect higher–molecular weight forms of Bik1p in this strain, even when Smt3p was overexpressed for 2 h (unpublished data).

We next investigated whether Pac1p would shift in the *ulp1*-ts strain. Unlike Bik1p, Pac1p displayed an extensive ladder of slower-migrating forms at the nonpermissive temperature (Figure 5, compare lanes 3 and 6). When additional Smt3p expression was induced, the level of shifted forms of Pac1p was pronounced even at the permissive temperature (compare lanes 1 and 4). Few shifted forms of Pac1p were observed in a wild-type *ULP1*+ strain prepared under the same conditions (compare lanes 9 and 12). These results suggest that these higher–molecular weight forms of Pac1p are caused either directly or indirectly by the presence of SUMO.
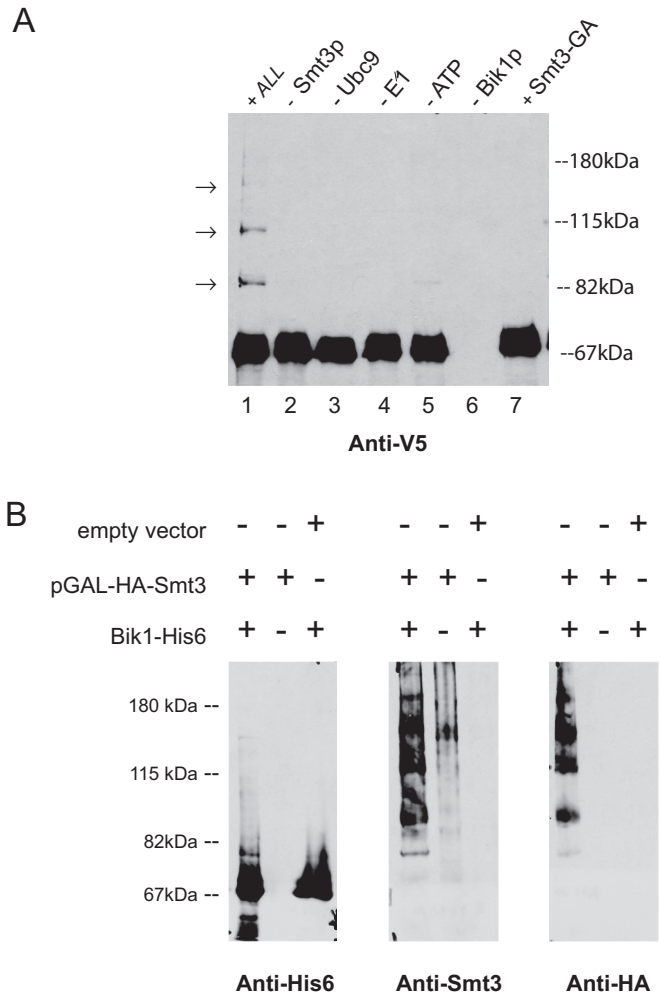

Anti-V5

FIGURE 4: Bik1p can be conjugated by Smt3p in vitro and in vivo. (A) Bik1p can be sumoylated in vitro. Bik1p was sumoylated using an in vitro assay described previously (Meednu *et al.*, 2008). Bik1p-V5-his6 (pRM5487) was purified from yeast, and the sumoylation enzymes were purified from bacteria (see *Materials and Methods*). The indicated components were mixed and incubated at 30°C for 2 h. The reactions were prepared for SDS–PAGE and Western blot analysis using anti-V5. Half of each reaction volume was run per lane. Bik1p-V5-his6 can be conjugated by Smt3p-GG in vitro (lane 1), as indicated by the shifted band (arrow). This band was always absent in reactions lacking Smt3p-GG (lane 2), Ubc9p (lane 3), and Aos1 (lane 4). A faint band of shifted Bik1p is observed when ATP is omitted from the reaction (lane 5). Bik1p also did not shift when Smt3-GA was used in the reaction (lane 7). (B) Bik1-his6 is shifted by the overexpression of Smt3p in vivo. Bik1-his6 (pRM5487) was purified from a yeast strain (yRM3350) either expressing HA-Smt3p (pRM5251) or containing an empty vector. Identical immunoblots were probed with anti-his6, polyclonal anti-Smt3p, or anti-HA.

SUMO chaining and ubiquitination contribute to Pac1p shifts

To determine whether the shift of Pac1p mobility was due to multiple monosumoylation events or polysumoylation, we mutated to arginine the three lysine residues within Smt3p that are required for chain formation (Bylebyl *et al.*, 2003). Analysis of the Pac1p shift using *SMT3*-K11R-K15R-K19R revealed that the higher–molecular weight smears were greatly reduced (Figure 6A, compare lanes 1 and 7). This suggests that polysumoylation contributes to the higher–molecular weight shifts of Pac1p.
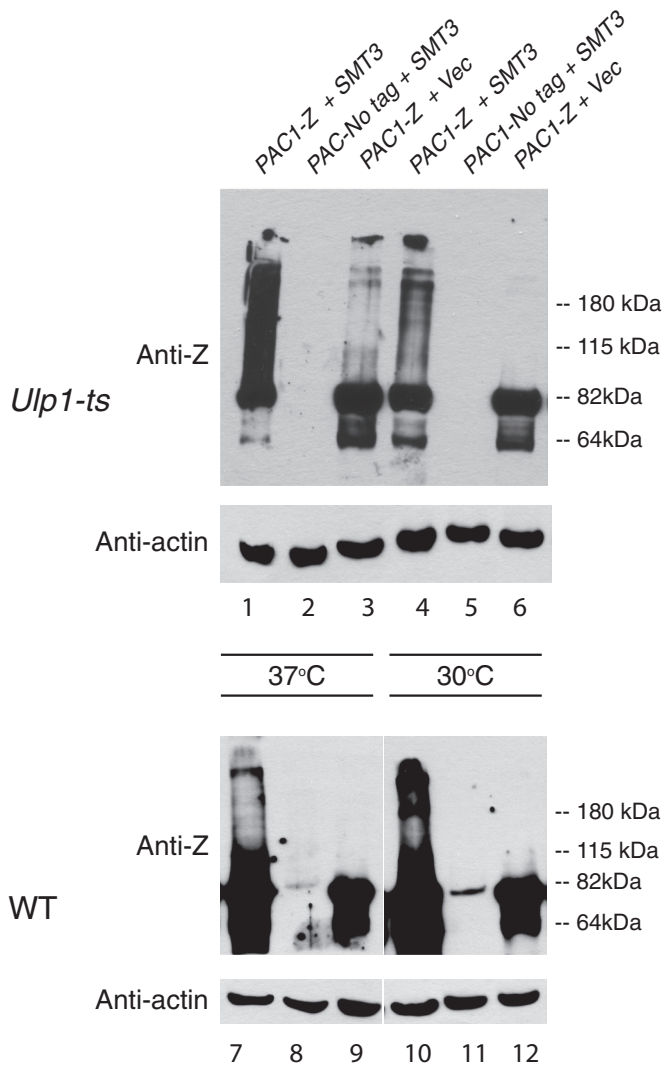
FIGURE 5: Inhibition of the SUMO protease Ulp1p shifts Pac1p in vivo. Whole-cell extracts were prepared as described in *Materials and Methods* from a *ulp1*-ts strain (yRM8139; top) or a wild-type strain (yRM3403; bottom) expressing Pac1p-4Z on a CEN plasmid under the control of its own promoter (pRM3573) and Smt3p under the control of a copper-inducible promoter (pRM8023). The appropriate empty CEN vectors allowed all strains to be grown in SC–ura–leu. Smt3p was induced for 2 h at the indicated temperatures. The white line in the Western blot of at the bottom indicates that this blot was rearranged to match the layout of the top. Lanes 7–9 are directly comparable to lanes 10–12. Rabbit anti-human immunoglobulin–horseradish peroxidase (IgG-HRP) antibody (Santa Cruz Biotechnology) was used to detect Pac1p-4Z. The stacker gel in this experiment was removed before immunoblotting.

Although Pac1p shifts in a Ulp1p-dependent manner, this does not eliminate the possibility that other modifications might also play a role. To test whether ubiquitin might also contribute to the shifts, we transformed a ubiquitin plasmid into the *ulp1*-ts strain containing Pac1p. This resulted in some higher–molecular weight bands of Pac1p, but the shift was not as extensive as when *SMT3* was present (Figure 6A, compare lanes 5 and 7). Taken together, these findings suggest that both polysumoylation and ubiquitination contribute to the higher–molecular weight forms of Pac1p.
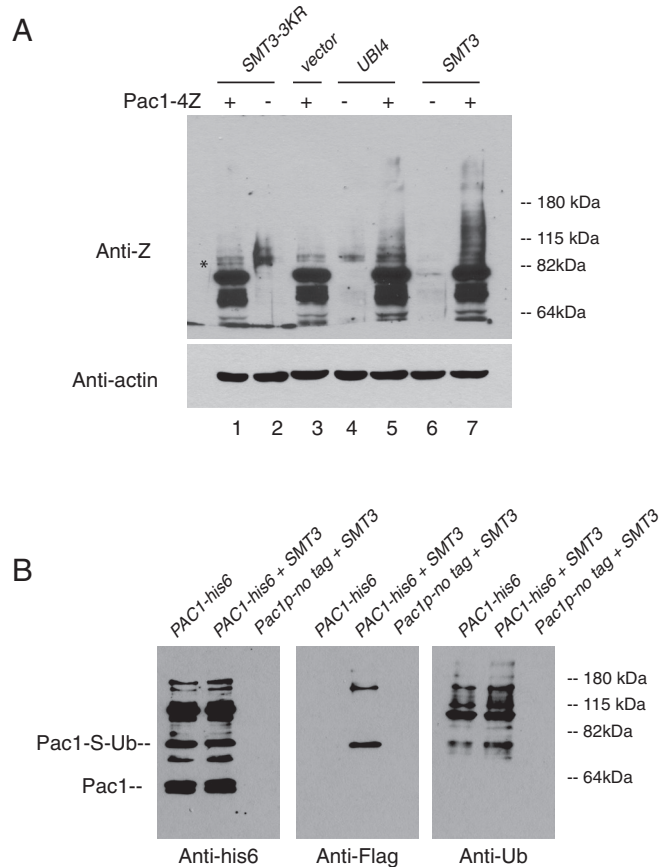

FIGURE 6: Both SUMO chaining and ubiquitination contribute to the higher–molecular weight forms of Pac1p. (A) The laddering effect of Pac1p is due to SUMO chain formation and ubiquitination. Plasmids expressing *SMT3gg*-his6-HA (pRM8023), *smt3gg-K11, 15, 19*R-his6-HA (*smt3*-3KR, pRM8836), or an empty *URA3* vector (pRM2205) were transformed into *ULP1*-TS strain (yRM8139). To induce the *SMT3* constructs, strains were treated with 1 mM CuSO₄ for 2 h at 37°C. Whole-cell lysates were prepared for each strain, as described in *Materials and Methods*, and analyzed by 8% SDS–PAGE. Membrane was immunoblotted with rabbit anti-human IgG-HRP antibody (Santa Cruz Biotechnology) to identify Pac1p-4Z. Pac1p laddering is due in part to ubiquitination. Plasmids expressing *UBI4*-myc (Ub, pRM8388) or an empty *URA3*-vector (pRM2205) were transformed into a *ULP1*-TS strain (yRM8139). Asterisk denotes a background band. *UBI4* encodes ubiquitin (Ub). In this experiment, the stacker gel was removed before immunoblotting. (B) SUMO and ubiquitin copurify with Pac1p. Pac1p-his6 (pRM9232) was integrated at the genomic *PAC1* locus of *ulp1*-TS strains. The resulting Pac1p-his6 is expressed at endogenous levels under its own promoter. These strains contained either FLAG-Smt3-GG (yRM8011) or an empty vector. The strains were shifted to 37°C for 2 h, and whole-cell extracts were prepared (14 ml at 1.4 mg/ml). Pac1p-his6 was purified from the cell extract using nickel beads, as described in *Materials and Methods*. The his6 epitope was detected using mouse anti-his6, Smt3p with mouse anti-FLAG, and ubiquitin with mouse anti-ubiquitin, as described in *Material and Methods*.

SUMO and ubiquitin copurify with Pac1p

To further explore whether the Pac1p shifts observed in the *ulp1*-ts strain are due to SUMO conjugation, we pulled down Pac1p-his6 on nickel beads from a yeast strain expressing Smt3-GG, the processed form (see *Materials and Methods*). The unmodified form of Pac1p appeared as a doublet, perhaps indicating that Pac1p is phosphory-lated. Four to seven higher–molecular weight forms of Pac1p were

observed after the pull down (Figure 6B). Two of these cross-reacted with anti-FLAG, which marks SUMO, indicating that these two shifts are due to SUMO conjugation of Pac1p (Pac1-S). To investigate whether the nonreactive bands might be due to another modification, we probed a third identical panel with anti-ubiquitin. This revealed that both of the anti-FLAG bands also reacted with anti-ubiquitin. These findings suggest that Pac1p is altered by at least two types of posttranslational modification—ubiquitin and SUMO. Moreover, two of the bands that were nonreactive with anti-FLAG did react with anti-ubiquitin. This suggests the possibility that some forms of Pac1p may contain only ubiquitin.

She1p and Kar9p inhibit the modification of Pac1p

Pac1p functions in the dynein pathway to help recruit dynein to the plus end of the cytoplasmic microtubule before its off-loading to the cortex (Li et al., 2005; Markus et al., 2011). To determine whether the integrity of the dynein pathway affects the modification of Pac1p, we examined Pac1p in several deletion strains related to various aspects of dynein function. KIP2 encodes a kinesin that transports Bik1p to the plus end of the microtubule (Carvalho et al., 2004). DYN1 encodes the dynein motor itself, and JNM1 encodes a component of the dynactin complex (McMillan and Tatchell, 1994). NDL1 encodes a NudE homologue that helps localize dynein to the plus end (Li et al., 2005; Moore et al., 2008). NUM1 encodes a cortical protein important for the off-loading of dynein (Heil-Chapdelaine et al., 2000; Farkasovsky and Küntzel, 2001). In a NUM1-deleted strain, the off-loading of dynein to the cortex is blocked (Lee et al., 2005). In each of these delete strains, little or no additional shift in Pac1p was observed (Figure 7A). We next tested a strain deleted for SHE1, which encodes a regulator of the dynein–dynactin interaction (Woodruff et al., 2009; Markus et al., 2011; Bergman et al., 2012). Surprisingly, Pac1p shifted significantly. This finding suggests that She1p is a novel inhibitor of Pac1p modifications.

To investigate further, we analyzed the shift of Pac1p in strains deleted for members of the Kar9 pathway, which orients the cytoplasmic microtubule into the bud (Miller and Rose, 1998; Miller et al., 1998). BIM1 encodes an EB1 homologue and microtubule-binding protein that binds Kar9p (Lee et al., 2000; Miller et al., 2000). KAR9 encodes a linker protein between BIM1 and the type V myosin Myo2p (Miller et al., 1999, 2000; Hwang et al., 2003). The movement of Myo2p along an actin cable serves to guide the attached microtubule into the bud (Beach et al., 2000; Yin et al., 2000). KIP3 encodes a type 8 kinesin in the Kar9 pathway that controls microtubule length (Miller et al., 1998; Su et al., 2011). Surprisingly, an increase was observed in the shift of Pac1p (Figure 7B). This suggests that the Kar9 pathway inhibits the interaction of Pac1p with Smt3p and/or ubiquitin. This is consistent with earlier findings that Bim1p interacts with She1p by two-hybrid analysis (Wong et al., 2007).

The results from Figure 7A could in theory be explained by She1p blocking the addition of either SUMO or ubiquitin. To distinguish between these two possible mechanisms, Pac1p-his6 from she1Δ and wild-type strains was enriched on nickel beads, and identical immunoblots were analyzed by probing with anti-SUMO or anti-ubiquitin (Figure 7C and 7C'). Consistently, larger amounts of Pac1p were purified from equal amounts of protein extract in the she1Δ and ulp1 strains than from wild type. This indicates, but does not prove, that these modifications may affect the steady-state stability of Pac1p. Furthermore, when anti-SUMO was used, nearly identical amounts of reactivity were observed in the she1Δ and wild-type (WT) strains. This suggests that increased sumoylation is not the cause of the higher–molecular weight forms of Pac1p observed in the she1Δ strains. However, when probed with anti-ubiquitin, additional reactivity was observed. This suggests that the addition of ubiquitin contributes to the higher forms of Pac1p seen in she1Δ. How She1p blocks this addition of ubiquitin remains an active avenue of further investigation.

PAC1 and BIK1 interact with WSS1, a SUMO isopeptidase, and NIS1-RIS1, a STUbL enzyme complex

SUMO-targeted ubiquitin ligases can link the sumoylation and ubiquitination pathways by ubiquitinating proteins already modified by sumoylation, thus promoting their removal by the proteasome (Sun et al., 2007; Uzunova et al., 2007; Xie et al., 2007). Wss1p was originally identified as a weak suppressor of a temperature-sensitive allele of Smt3p (Biggins et al., 2001). Recently Wss1p was shown to be a SUMO-dependent isopeptidase that promotes the targeting of SUMO-conjugated proteins to the proteasome (Mullen et al., 2010). Our previous work showed that Kar9p interacted with both WSS1 and the complex encoded by the RIS1 and NIS1 genes (Meednu et al., 2008). Therefore we tested whether Bik1p or Pac1p would also interact with the STUbL enzyme Nis1p–Ris1p and the SUMO iospeptidase Wss1p by two-hybrid analysis. Indeed, both did (Figure 8A).

These findings suggest the possibility that the shifts of Pac1p may be modulated by a STUbL enzyme and the proteasome. If such a model is correct, higher–molecular weight forms of Pac1p should be present when the STUbL is absent from the cell. To assess this, we examined the levels of shifted Pac1p in strains deleted for WSS1, RIS1–NIS1, or another STUbL enzyme complex, SLX5–SLX8. As shown in Figure 8B, the shifted forms of Pac1p were significantly increased in strains lacking the catalytic subunit of the STUbL Ris1p and the Wss1p isopeptidase. No difference in the shift pattern was detected in strains deleted for SLX5 or SLX8, suggesting that the shift in Pac1p is specific to only one of the two STUbLs present in yeast. These findings also indicate that Pac1p may be a substrate of the Ris1p STUbL enzyme. Further work is required to determine whether STUbLs can exert an effect on the unmodified levels and/or steady-state levels of Pac1p.

Together these results suggest the possibility that ubiquitination of Pac1p by the Nis1p–Ris1p STUbL modulates the turnover of sumoylated Pac1p. Wss1p may aid in the delivery to or the processing of Pac1p by the proteasome. To investigate this, we treated cells with a proteasome inhibitor, MG132. Because yeast cells can pump the MG132 drug out of the cell, this study was conducted in a strain deleted for PDR5, which encodes a drug pump (Fleming et al., 2002). As seen Figure 8C, higher–molecular weight forms of Pac1p are present in the stacker portion of the gel when the proteasome is inhibited with MG132 (compare lanes 2 and 3, asterisk). Taken together, these results suggest that the STUbL enzyme Nis1p–Ris1p controls the levels of posttranslational modifications attached to Pac1p.

DISCUSSION

In this study, we show that the Lis1 homologue Pac1p and the CLIP-170 homologue Bik1p interact with SUMO and several enzymes of the SUMO modification pathway. Pac1p also interacts with ubiquitin. We also show that Bik1p and Pac1p interact with the STUbL enzyme Nis1p–Ris1p and that the posttranslational modifications of Pac1p are controlled by this STUbL enzyme. In summary, we showed that two new classes of conserved microtubule-associated proteins interact with and are likely to be regulated by SUMO. With this work, four different spindle-positioning proteins have now been shown to interact with SUMO.
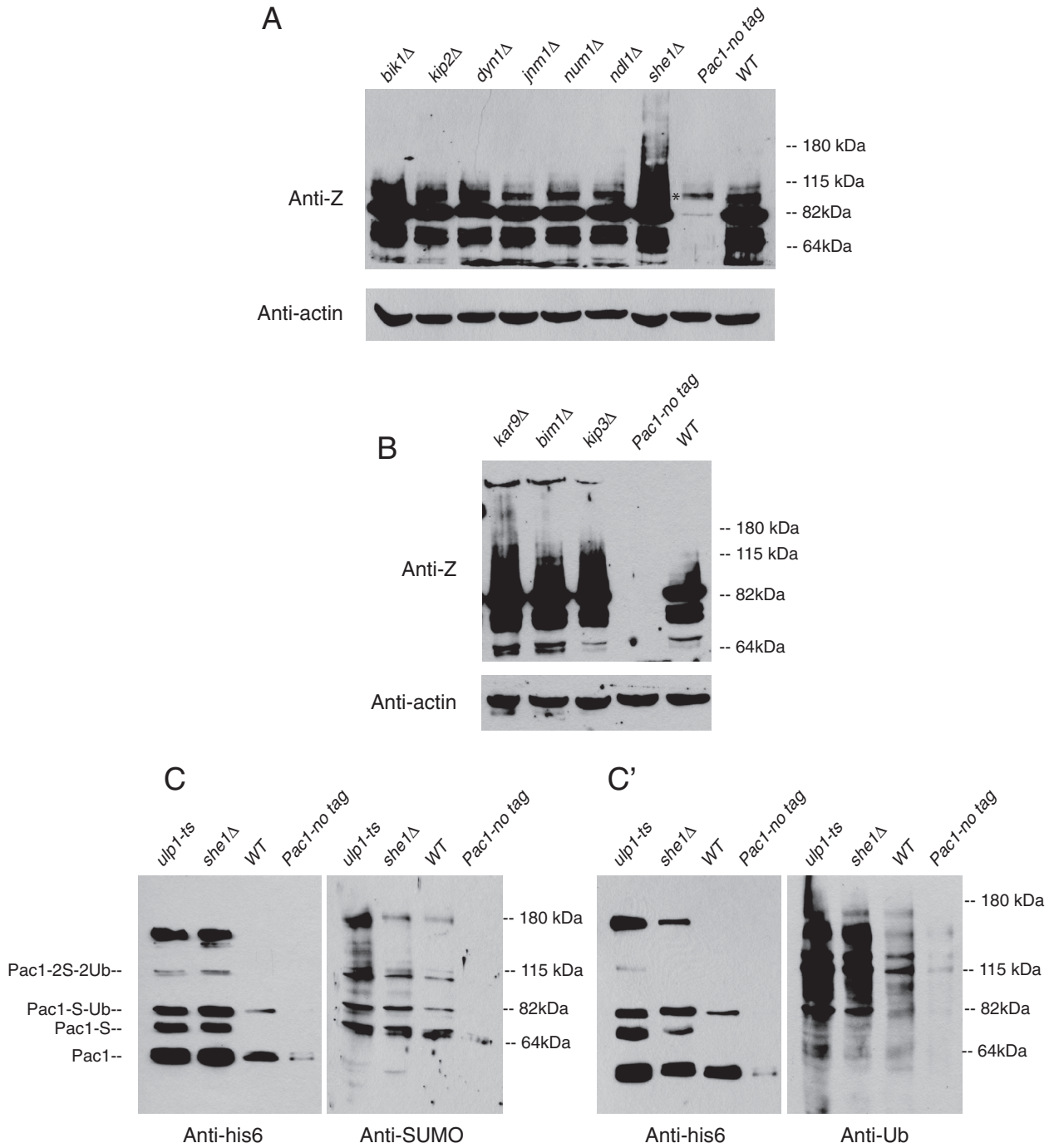
A

bik1Δ kip2Δ dyn1Δ jnm1Δ num1Δ ndl1Δ she1Δ Pac1-no tag WT

Anti-Z

-- 180 kDa
-- 115 kDa
*
-- 82kDa
-- 64kDa

Anti-actin

B

kar9Δ bim1Δ kip3Δ Pac1-no tag WT

Anti-Z

-- 180 kDa
-- 115 kDa
-- 82kDa
-- 64kDa

Anti-actin

C

ulp1-ts she1Δ WT Pac1-no tag   ulp1-ts she1Δ WT Pac1-no tag

Pac1-2S-2Ub--
Pac1-S-Ub--
Pac1-S--
Pac1--

-- 180 kDa
-- 115 kDa
-- 82kDa
-- 64kDa

Anti-his6   Anti-SUMO

C'

ulp1-ts she1Δ WT Pac1-no tag   ulp1-ts she1Δ WT Pac1-no tag

-- 180 kDa
-- 115 kDa
-- 82kDa
-- 64kDa

Anti-his6   Anti-Ub

FIGURE 7: She1p and Kar9p inhibit Pac1p modification. (A) Strains deleted for *SHE1* in the dynein pathway display higher–molecular weight forms of Pac1p. Strains deleted for *BIK1* (yRM3350), *KIP2* (yRM3355), *DYN1* (yRM3346), *JNM1* (yRM7116), *NUM1* (yRM3137), *NDL1* (yRM9050), *SHE1* (yRM9051), and WT (yRM3403) were transformed with plasmids expressing Pac1p-4z (pRM3573) or nontagged Pac1p (pRM3574). Whole-cell lysates were prepared from each strain, as described in *Materials and Methods*, and analyzed by 8% SDS–PAGE. Rabbit anti-human IgG-HRP antibody (Santa Cruz Biotechnology) was used for detection of Pac1p-4z. An asterisk is used to denote a background band revealed in the Pac1-no-tag control lane. (B) Kar9p inhibits the shift of Pac1p. Whole-cell extracts prepared from strains deleted for *KAR9* (yRM3404), *BIM1* (yRM3352), *KIP3* (yRM3140), and WT (yRM3403) were transformed with plasmids expressing Pac1p-4z (pRM3573) or nontagged Pac1p (in WT; pRM3574). Rabbit anti-human IgG-HRP antibody was used for detection. (C) She1p inhibits the ubiquitination of Pac1p. Pac1p was tagged with his6 by integrating the C-terminally tagged construct ΔN-Pac1-his6 (pRM9232) to produce Pac1p-his6 expressed at endogenous levels under its own promoter. Pac1p-his6 was purified on nickel beads from equal amounts of protein extract (14 ml at 1.6 mg/ml) prepared from the indicated strains, *ulp1*-ts (yRM8139), *she1*Δ (yRM9051), and WT (yRM3403), grown at 30°C. Mouse anti-his6 was used to detect the his6 epitope. Smt3p was detected with rabbit anti-smt3, and ubiquitin with mouse anti-ubiquitin, as described in *Materials and Methods*. Note that the pattern of shifted Pac1p appears slightly different in this pull down than in Figure 6B because the pull downs were performed at different temperatures.

A

	WSS1	RIS1 / ULS1	NIS1	empty-AD	WSS1	RIS1 / ULS1	NIS1	empty-AD
PAC1								
BIK1								
empty-BD								

-His   -Ura-Leu

B

ris1Δ wss1Δ slx5Δ slx8Δ pac1-no tag WT

Anti-Z

-- 180 kDa
-- 115 kDa
-- 82kDa
-- 64kDa

Stacker

Anti-actin

1   2   3   4   5   6   7

C

no treatment DMSO MG132 PAC1-no tag PAC1-4-Z

pdr5Δ   WT

Anti-Z

*

Stacker

-- 180 kDa
-- 115 kDa
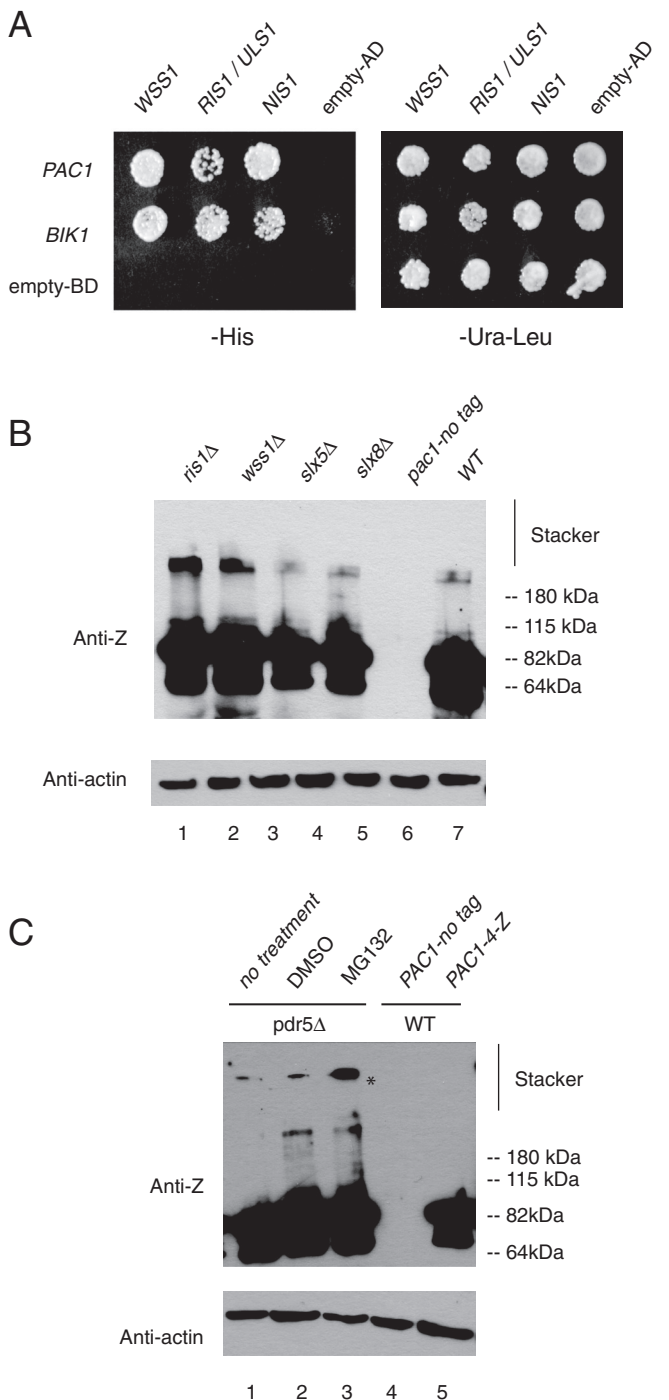-- 82kDa
-- 64kDa

Anti-actin

1   2   3   4   5

FIGURE 8: A STUbL complex alters Pac1p modification. (A) Pac1p interacts with the STUbL enzyme Nis1p–Ris1p and the SUMO isopeptidase Wss1p. *BIK1-BD* and *PAC1-BD* were tested for interaction against the SUMO peptidase encoded by *WSS1* (pRM4597) and the STUbL complex composed of *RIS1* (pRM4596), *NIS1 (pRM4595),* or empty AD (pRM4380). Diploids were selected on media lacking uracil and leucine (–ura–leu) and assayed for interactions on media lacking histidine (–his). (B) Strains deleted for the Ris1p STUbL display higher-molecular weight forms of Pac1p. Strains deleted for *RIS1* (yRM8574), *WSS1* (yRM4636), *SLX5* (yRM7887), *SLX8* (yRM7888), and WT (yRM3403) were transformed with a plasmid expressing Pac1-4Z (pRM3573) and nontagged Pac1p (pRM3574). Whole-cell extracts from the yeast strains were resolved by 8% SDS–PAGE and analyzed by anti-Z immunoblotting. An increase in SUMO conjugate levels can be seen in the *ris1Δ* and *wss1Δ* mutant

We use several different approaches to show that Pac1p interacts with SUMO. First, the two-hybrid analysis shows that Pac1p interacts with the GG but not the GA form of SUMO. This implies, but does not prove, that the interaction is due to a conjugation event. Second, inhibition of the SUMO-specific protease Ulp1p results in higher–molecular weight forms of Pac1p. This suggests that at least some of the higher–molecular weight forms are caused by SUMO moieties conjugated onto Pac1p. Indeed, when an additional SUMO is provided to the cell on a plasmid, a similar but significantly stronger banding pattern is seen. The higher–molecular weight forms of Pac1p are likely due to poly-SUMO chain formation, because the shifts are greatly diminished by the presence of a nonchainable form of SUMO. Pac1p also interacts with the STUbL enzyme Nis1p–Ris1p, an enzyme that recognizes sumoylated proteins. A pull-down assay with Pac1p suggests that the higher–molecular weight forms of Pac1p contain covalently attached SUMO. Taken together, these experiments strongly support our assertion that Pac1p is conjugated with SUMO.

Our conclusion that the interaction of Pac1p with SUMO may also involve cross-talk with ubiquitin is derived from four lines of investigation. First, we see a weak two-hybrid interaction of *PAC1* with ubiquitin, encoded by *UBI4*. Pac1p is also likely to be modified by ubiquitin, because higher–molecular weight forms of Pac1p can be generated by the inclusion of a plasmid encoding ubiquitin. Third, ubiquitin copurifies with Pac1p, with some shifted bands cross-reacting with both anti-ubiquitin and anti-SUMO. Fourth, Pac1p interacts with the ubiquitin ligase complex, Ris1p–Nis1p, and deletion of *RIS1* results in higher–molecular weight forms of Pac1p. This is consistent with our previous finding that Kar9p and Bim1p interact with Wss1p and the same STUbL (Meednu *et al.*, 2008). The finding that multiple spindle-positioning proteins interact with SUMO suggests the possibility that the Nis1p–Ris1p STUbL enzyme may regulate spindle positioning.

This is the first report that a member of the Lis1 family or a member of the CAP-Gly domain family is modified by SUMO. This has significant implications for the regulation of these two classes of microtubule-associated proteins, which are widely conserved across evolution. Prior to this work, only four other microtubule-associated proteins have been shown to be modified by SUMO. These are Tau (Dorval and Fraser, 2006; Takahashi *et al.*, 2008), Ndc80p (Montpetit *et al.*, 2006), CENP-E (Zhang *et al.*, 2008), and Kar9p (Leisner *et al.*, 2008; Meednu *et al.*, 2008). We also showed that the EB1 homologue Bim1p interacts with SUMO by two-hybrid analysis, but details of this interaction and whether this interaction represents an actual conjugation by SUMO remain to be elucidated (Meednu *et al.*, 2008). Our findings are also notable in that Pac1p was not found in any of the previous genome-wide screens for sumoylated proteins (Zhou *et al.*, 2004), indicating that yeast SUMO-ome may not yet be complete.

Previous reports suggest that the Kar9 pathway for spindle positioning is regulated by sumoylation (Leisner *et al.*, 2008; Meednu *et al.*, 2008). Leisner *et al.* (2008) showed that the spindle-positioning defect seen in the nonsumoylatable *kar9*-4K-R mutant is not as severe as the *smt3-331* defect. This suggests that there are

cells compared with WT. (C) Inhibition of the proteasome results in accumulation of higher–molecular weight forms of Pac1p. Plasmids expressing Pac1p-4z (pRM3573) or nontagged Pac1p (pRM3574) were transformed into WT (yRM3403) and *pdr5Δ* (yRM8571) strains. Cells were treated at 30°C for 2 h with dimethyl sulfoxide (DMSO) alone or 50 μM MG132 (dissolved in DMSO) or not treated, as indicated. Whole-cell lysates were prepared as described in *Materials and Methods* and analyzed by 8% SDS–PAGE for anti–Pac1p-4z.
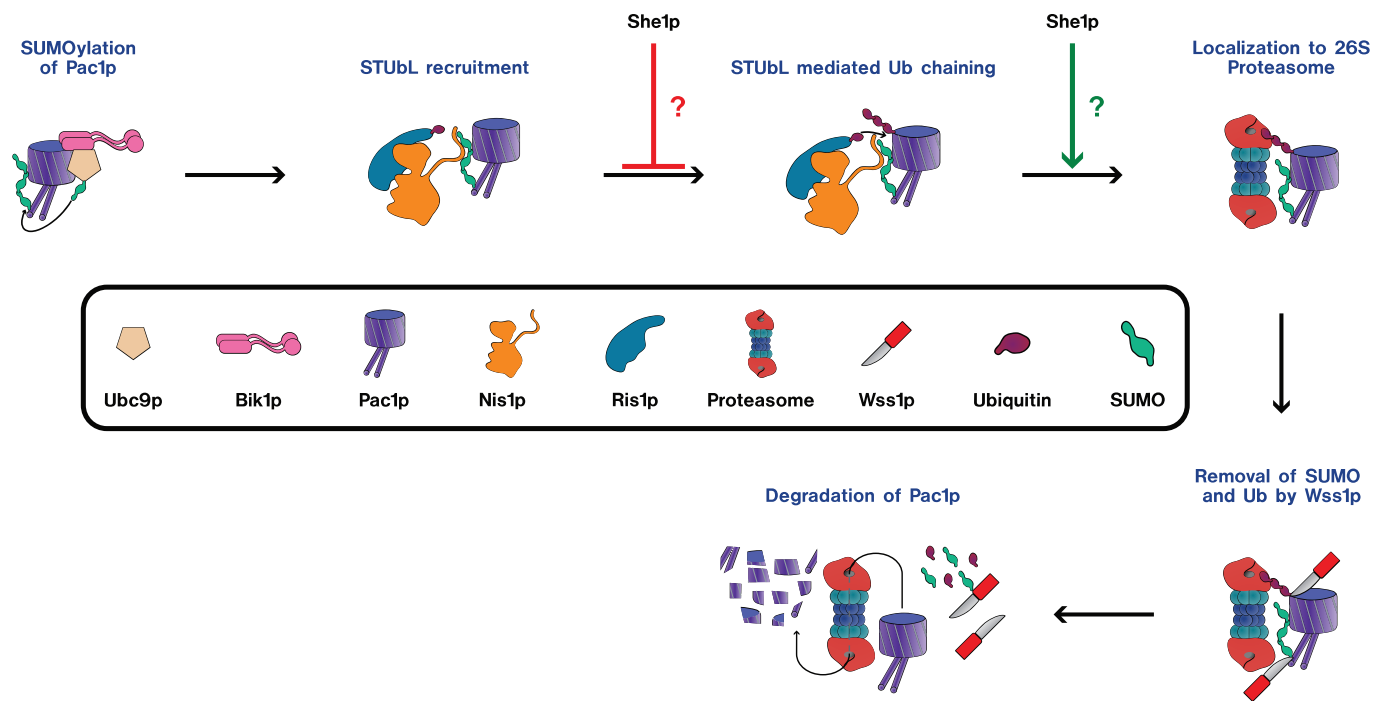
FIGURE 9: Model of Bik1p and Pac1p interaction with a STUbL and Wss1p.

additional proteins required for spindle positioning that are also regulated by sumoylation. The findings reported here suggest that Pac1p and/or Bik1p may be the additional protein(s). Thus it is likely that both spindle-positioning pathways in yeast may be regulated by sumoylation. Future studies should elucidate whether this signal transduction system regulates each pathway separately or whether they are coordinated as a unit.

Our two-hybrid bridging data suggest that Bik1p and Pac1p are both required for their mutual interaction with SUMO and Ubc9p. However, this relationship was not observed in the in vitro shift assay using purified Bik1p. This suggests that Pac1p is not required for the in vitro shift of Bik1p. The apparent discrepancy between the two assays may be reconciled if Pac1p enhances the sumoylation of Bik1p. Consistent with this idea is our observation that Bik1p from partially fractionated extracts shifted better in vitro than purified Bik1p (unpublished data). Future work to test this hypothesis is warranted.

Furthermore, the bridging data in which Bik1p is required for the Wss1p's interaction with Pac1p (but not vice versa) suggest that Bik1p may recruit Wss1p to the Bik1p–Pac1p complex (Figure 9). This is consistent with our data that Pac1p is hypermodified in a strain deleted for *WSS1*.

We propose a model in which Pac1p sumoylation and its subsequent interaction with a STUbL promotes its degradation via the proteasome (Figure 9). In this model, Wss1p aids in debranching of polysumoylated and/or polyubiquitinated Pac1p at the proteasome. Because She1p regulates the association of dynactin with dynein (Woodruff et al., 2009), our finding that She1p inhibits the modification of Pac1p suggests the possibility that sumoylation and/or ubiquitination may regulate the interaction of dynein with its accessory proteins. In our model, She1 protein blocks the ubiquitination of Pac1p. It might also promote the proteasome-mediated degradation of modified Pac1p. We speculate that the sumoylation of Pac1p may play a role in regulating the off-loading of dynein to the cell cortex.

Several questions remain. SUMO is induced by various types of cellular stress. Future work is needed to show whether the sumoylation of these key classes of microtubule-associated proteins represents a mechanism by which microtubule-dependent processes are inactivated under conditions that are inhospitable for cell division. Furthermore, both Pac1p and Lis1 serve as adaptors of dynein. Lis1 regulates some but not all of dynein's functions. It remains to be determined whether Lis1, either in neurons or epithelial cells, is also sumoylated. Our findings have implications for how this class of dynein adaptor may regulate dynein function. Because dynein is critical to a number of fundamental processes important for life, it will be important for future studies to elucidate the widespread utility of this modification in other systems.

MATERIALS AND METHODS
Two-hybrid analysis
Two-hybrid analysis was carried out as previously described (Moore and Miller, 2007; Moore et al., 2008 ; Meednu et al., 2008). All analysis was carried out after 2–3 d of growth at 30°C. *PAC1*-DNA-binding domain (BD) was constructed by amplifying *PAC1* from pRM3574/pJG13 with *Bam*HI and *Pst*I ends and ligating it into pRM1154/GBDU-C1 cleaved with the same enzymes. This generated pRM3604 (Table 1), which was sequenced to confirm the absence of unintended PCR errors.

PAC1 was deleted from the two-hybrid reporter strain yRM1757 by one-step gene replacement using a PCR product derived from genomic DNA from the *pac1Δ::KAN*[R] deletion strain (Open Biosystems, Huntsville, AL), yRM3138. This generated pRM6249, which was confirmed by PCR.

BIK1-BD was generated by excising the *BIK1* coding fragment with *Eco*RI and *Bam*HI from pRM2627 and ligating it to the BD vector, pRM1156, cut with the same enzymes. This generated pRM4924.

Yeast strain	Genotype/comments	Source
yRM1756/PJ69-4α	*MATα trp1-901 leu2-3 leu2-112 ura3-52 his3Δ200 gal4Δ gal80Δ LYS2::GAL1-HIS3 GAL2-ADE2 met2::GAL7-lacZ*	James *et al.* (1996)
yRM1757/PJ69-4A	*MATa trp1-901 leu2-3 leu2-112 ura3-52 his3Δ200 gal4Δ gal80Δ LYS2::GAL1-HIS3 GAL2-ADE2 met2::GAL7-lacZ*	James *et al.* (1996)
yRM2057	*MATa bim1Δ::KAN trp1-901 leu2-3 leu2-112 ura3-52 his3Δ200 gal4Δ gal80Δ LYS2::GAL1-HIS3 GAL2-ADE2 met2::GAL7-lacZ*	Miller *et al.* (2000)
yRM2258	*MATa bik1Δ::TRP trp1-901 leu2-3 leu2-112 ura3-52 his3Δ200 gal4Δ gal80Δ LYS2::GAL1-HIS3 GAL2-ADE2 met2::GAL7-lacZ*	Moore *et al.* (2006)
yRM3137	*MATa num1Δ::KAN his3Δ leu2Δ met15Δ ura3Δ*	Open Biosystems
yRM3138	*MATa pac1Δ::KAN his3Δ leu2Δ met15Δ ura3Δ*	Open Biosystems
yRM3140	*MATa kip3Δ::KAN his3Δ leu2Δ met15Δ ura3Δ*	Open Biosystems
yRM3346	*MATa dyn1Δ::KAN his3Δ leu2Δ met15Δ ura3Δ*	Open Biosystems
yRM3350	*MATa bik1Δ::KAN his3Δ leu2Δ met15Δ ura3Δ*	Open Biosystems
yRM3352	*MATa bim1Δ::KAN his3Δ leu2Δ met15Δ ura3Δ*	Open Biosystems
yRM3355	*MATa kip2Δ::KAN his3Δ leu2Δ met15Δ ura3Δ*	Open Biosystems
yRM3403	*MATa his3Δ1 leu2Δ1 met15Δ ura3Δ*	This study
yRM3404	*MATa kar9Δ::KAN his3Δ leu2Δ met15Δ ura3Δ*	Open Biosystems
yRM4636	*MATa wss1Δ::KAN his3Δ leu2Δ met15Δ ura3Δ*	Open Biosystems
yRM6172	*MATa kar9Δ::KAN trp1-901 leu2-3 leu2-112 ura3-52 his3Δ200 gal4Δ gal80Δ LYS2::GAL1-HIS3 GAL2-ADE2 met2::GAL7-lacZ*	Meednu *et al.* (2008)
yRM6249	*MATa pac1Δ::KAN[R] trp1-901 leu2-3 leu2-112 ura3-52 his3Δ200 gal4Δ gal80Δ LYS2::GAL1-HIS3 GAL2-ADE2 met2::GAL7-lacZ*	This study
yRM6444	*MATα bik1ΔC40::TRP1^{+} trp1-901 leu2-3 leu2-112 ura3-52 his3Δ200 gal4Δ gal80Δ LYS2::GAL1-HIS3 GAL2-ADE2 met2::GAL7-lacZ*	This study
yRM7205	*MATa bik1Δ::KAN[R] leu2Δ ura3Δ his3Δ met15Δ {pRM5487 = pGAL-BIK1-his6 AmpR URA3}*	This study
	{pRM5251 = pGAL-3HA-FLAG-SMT3 Amp[R] HIS3}	
yRM7116	*MATa jnm1Δ::KAN his3Δ leu2Δ met15Δ ura3Δ*	Open Biosystems
yRM7213	*MATa bik1Δ::KAN[R] leu2Δ ura3Δ his3Δ met15Δ*	This study
	{pRM5251 = pGAL-3HA-FLAG-SMT3 Amp[R] HIS3}	
yRM7600	*MATa bik1Δ::KAN[R] leu2Δ ura3Δ his3Δ met15Δ*	This study
	{pRM5487 = pGAL-BIK1-his6 AmpR URA3}	
	{pRM4878 = pESC HIS3 with c-myc eliminated}	
yRM7887	*MATa slx5Δ::KAN his3Δ leu2Δ met15Δ ura3Δ*	Open Biosystems
yRM7888	*MATa slx8Δ::KAN his3Δ leu2Δ met15Δ ura3Δ*	Open Biosystems
yRM8011/YOK428	*MATα ulp1::KAN ulp1[ts]-NAT-TRP his3Δ1 leu2Δ ura3Δ {pRS425 GPD flag-SMT3-gg LEU2 2μ Amp[R]}*	Elmore *et al.* (2011)
yRM8012/YOK430	*MATα ulp1::KAN ulp1[ts]-NAT-TRP his3Δ1 leu2Δ ura3Δ {pRS425 GPD-SMT3-gg LEU2 2μ Amp[R]}*	Elmore *et al.* (2011)
yRM8139	*MATαulp1::KAN ulp1[ts]-NAT-TRP his3Δ1 leu2Δ ura3Δ*	This study
yRM8571	*MATa pdr5Δ::KAN his3Δ leu2 Δ met15 Δ ura3 Δ*	Open Biosystems
yRM8574	*MATa ris1Δ::KAN his3Δ leu2 Δ met15 Δ ura3 Δ*	Open Biosystems
yRM9050	*MATa ndl1Δ::KAN his3Δ leu2Δ met15Δ ura3Δ*	Open Biosystems
yRM9051	*MATa she1Δ:: KAN his3Δ leu2Δ met15Δ ura3Δ*	Open Biosystems
yRM9248	*MATα ulp1::KAN ulp1[ts]-NAT-TRP his3Δ1 leu2Δ ura3Δ PAC1::his6:: HIS3+ {pRS524 GPD-FLAG-Smt3-gg-LEU2 2 μ Amp[R]}*	This study

TABLE 1: Strains and plasmids used in this study.

Plasmid	Genotype/comments	Source
pRM1151	*GAD empty LEU2 2μ* Amp[R]	James *et al.* (1996)
pRM1154	*GBDU* empty *URA3 2μ* Amp[R]	James *et al.* (1996)
pRM1493	*GBDU-KAR9 URA3 2μ* Amp[R]	Miller *et al.* (2000)
pRM2200/pRS415	*LEU2 CEN* Amp[R]	Sikorski and Hieter (1989)
pRM2205/pRS426	*URA3 2μ* Amp[R]	Sikorski and Hieter (1989)
pRM2627	*GAD-BIK1 LEU2 2μ* Amp[R]	Moore *et al.* (2006)
pRM2908	*pGAL URA3 2μ* Amp[R]	This study
pRM3573/pJG423	*PAC1-4Z CEN6 LEU2* Amp[R]	Sheeman *et al.* (2003)
pRM3574/pJG213	*PAC1 CEN6 LEU2* Amp[R]	Sheeman *et al.* (2003)
pRM3595	*GBDU-KIP2 URA3 2μ* Amp[R]	Meednu *et al.* (2008)
pRM3604	*GBDU-PAC1 URA3 2μ* Amp[R]	This study
pRM4380	*GAD424 LEU2 2μ* Amp[R]	Meednu *et al.* (2008)
pRM4382/pLAJ20	*GAD-SMT3-GG LEU2 2μ* Amp[R]	Meednu *et al.* (2008)
pRM4383/pLAJ21	*GAD-SMT3-GA LEU2 2μ* Amp[R]	Meednu *et al.* (2008)
pRM4495	*GAD-UBC9 LEU2 2μ* Amp[R]	Meednu *et al.* (2008)
pRM4496	*GAD-NFI1 LEU2 2μ* Amp[R]	Meednu *et al.* (2008)
pRM4595	*GAD-NIS1 LEU2 2μ* Amp[R]	Meednu *et al.* (2008)
pRM4596	*GAD-RIS1/ ULS1 LEU2 2μ* Amp[R]	Meednu *et al.* (2008)
pRM4597	*GAD-WSS1 LEU2 2μ* Amp[R]	Meednu *et al.* (2008)
pRM4920/pLAJ19	*GAD-SMT3 LEU2 2μ* Amp[R]	Meednu *et al.* (2008)
pRM4924	*GBDU-BIK1 URA3 2μ* Amp[R]	This study
pRM5169	*his6-UBC9* Amp[R]	Johnson and Blobel (1997)
pRM5251	*pGAL-3HA-FLAG-SMT3 HIS3* Amp[R]	This study
pRM5487	*pGAL-BiK1-V5-his6 URA3* Amp[R]	This study
pRM5829	*GAD-URM1 LEU2 2μ* Amp[R]	Meednu *et al.* (2008)
pRM5880.	*GAD-UBI4 LEU2 2μ* Amp[R]	Meednu *et al.* (2008)
pRM6713	*his6-S-tag-Smt3p-gg Kan[R]*	This study
pRM6760	*GST-AOS1/UBA2 2μ* Amp[R]	Bencsath *et al.* (2002)
pRM8023	*Cu²⁺ promoter - HA-his6-SMT3-gg URA3 2μ* Amp[R]	Elmore *et al.* (2011)
pRM8388/pUB175	*Cu²⁺ promoter - myc-UBI4 URA3 2μ* Amp[R]	Finley *et al.* (1989)
pRM8836	*Cu2+ promoter - HA- his6-smt3-gg-K11R-K15R-K19R URA3 2μ* Amp[R]	This study
pRM9232	*ΔN-Pac1-his6 HIS3 YIP* Amp[R]	This study

TABLE 1: Strains and plasmids used in this study. Continued

In vitro sumoylation

Bik1p was sumoylated using a previously described protocol (Meednu *et al.*, 2008). Strains expressing Bik1p-V5-his6 were grown at 30°C in synthetic complete (SC) media lacking uracil (–ura) containing 2% sucrose, and Bik1p expression was induced by the addition of 2% galactose for 2 h. To prepare yeast extracts, cells were washed once with water, resuspended in cold 1× binding buffer (20 mM Tris-HCl, pH 7.9, 5 mM imidazole, 0.5 M NaCl) containing 0.2% protease inhibitor P8215 (Sigma-Aldrich, St. Louis, MO) and 1 mM phenylmethylsulfonyl fluoride (PMSF; Sigma-Aldrich). Cells were lysed by vortexing with glass beads. Crude extracts were clarified by centrifugation at 13,000 rpm for 30 min, applied to nickel resin (Novagen/EMD, Darmstadt, Germany), and washed with 25 column volumes of 1× binding buffer containing 50 mM imida-zole. Bound protein was eluted with 1× binding buffer containing 300 mM imidazole and dialyzed overnight into sumoylation assay buffer (50 mM Tris, pH 7.6, 5 mM MgCl₂, 15% glycerol) at 4°C.

Sumoylation enzymes were purified from bacteria as previously described (Meednu *et al.*, 2008). Briefly, the processed form of SUMO his6-Smt3p-GG (pRM6713) and Ubc9p-his6 (pRM5169) were purified from bacteria using nickel affinity chromatography (Johnson and Blobel, 1997). The E1 components, Aos1p and Uba2p, located on a polycistronic plasmid (pRM6760) were copurified from bacteria using glutathione affinity chromatography (Bencsath *et al.*, 2002). The assay was carried out using purified sumoylation enzymes (2 μg of Smt3p-his6, 1 μg of Ubc9p-his6, 1 μg of GST-Uba2p/Aos1p) mixed with Bik1p-V5-his6 (1 μg) in the presence and absence of ATP and an ATP regeneration system at 30°C for 2 h.

Bik1p in vivo shift assay

Yeast strains (yRM3350) containing pGAL-BIK1-his6 (pRM5487) and 3HA-FLAG-SMT3 (pRM5251) or an empty pGAL plasmid (pRM2908) were grown to mid–exponential phase in SC media lacking uracil and histidine (–ura –his) containing 2% sucrose and then induced with 2% galactose. Extracts were prepared by disrupting cells with glass beads, followed by centrifugation at 13,000 rpm in a 4°C cold room for 30 min. Bik1p was enriched from 3 mg of extract on a nickel column resin (Novagen/EMD). Beads were washed eight times with B150 buffer and twice with B150 buffer (50 mM Tris, pH 7.4, 150 mM NaCl, 0.2% Triton X-100) containing 50 mM imidazole (Sigma-Aldrich). Bound proteins were eluted by the addition of 50 μl of 3× Laemmli buffer and boiled for 5 min. Samples were analyzed by SDS–PAGE (8%) and immunoblotting. Bik1-his6 was detected with mouse anti-his6 (Novagen/EMD). HA-tagged proteins were detected using mouse anti-HA (Santa Cruz Biotechnology, Santa Cruz, CA), and Smt3p was detected with rabbit anti-Smt3p. Secondary antibodies were obtained from Santa Cruz Biotechnology.

Preparation of whole-cell extracts in *ulp1*-ts strains.

Strains expressing *SMT3* under the control of a copper-inducible promoter (pRM8023) were grown to mid–exponential phase to an OD_{600} of <0.4 in liquid SC media lacking uracil and leucine (–ura –leu). Cells were shifted to either 30 or 37°C and simultaneously induced for *SMT3* expression by the addition of 1 mM $CuSO_4$ for 2 h. Cells were collected by low-speed centrifugation, washed, and resuspended in cold B150 breaking buffer; excess fluid was removed, and cells were resuspended in B150 breaking buffer containing 1 mM PMSF, 20 mM *N*-ethylmaleimide, 20 mM 2-iodoacetamide, and 1% Sigma-Aldrich protease inhibitor. Cells were lysed by vortexing with glass beads for 10 min. It should be noted that the inclusion of the alkylating agent 2-iodoacetamide was crucial for obtaining consistent results. Extracts were clarified by centrifugation at $13,000 \times g$ for 20 min at 4°C. Protein concentrations were determined by Bradford Protein Assay (Bio-Rad, Hercules, CA) using bovine serum albumin as a standard.

Pull-down assay

Yeast extracts were prepared as described earlier by bead beating cells in binding buffer (20 mM Tris-HCl, pH 7.9, 0.3 M NaCl, 10 mM imidazole, 1% protease inhibitor [#P8849; Sigma-Aldrich]). The volume was increased to 14 ml with binding buffer. Extracts were incubated with nickel beads at 4°C on a rotisserie for 1 h. Beads were collected and washed 7× with cold binding buffer containing 50 mM imidazole and 0.5 M NaCl. Samples were prepared for SDS–PAGE and Western blot analysis. The his6 epitope was detected using mouse anti-his6 (Novagen, Madison, WI) at 1:1500 in Tris-buffered saline (TBS) for 3 h at RT. Smt3p was detected using anti-Smt3p (Rockland, Gilbertsville, PA) at 1:2000 in phosphate-buffered saline (PBS) for 3 h at RT. Mouse anti-ubiquitin was obtained from Covance (Princeton, NJ) and used at 1:1500 in TBS for 3 h at room temperature. FLAG-tagged Smt3p was detected using mouse anti-FLAG (#3165; Sigma-Aldrich) at 1:5000 in TBS for 3 h at room temperature.

Western blotting

Western blotting was carried out using 8% SDS–PAGE as previously described (Moore *et al.*, 2006; Meednu *et al.*, 2008), except that 0.2% Tropix I-Block reagent (Applied Biosystems, Foster City, CA) with 0.1% Tween-20 in TBS was used as the blocking agent.

Plasmid construction

Nonchainable SUMO. Point mutations to generate lysine-to-arginine substitutions were introduced into HA-his6-Smt3 plasmid (pRM8023) by site-directed mutagenesis using the QuikChange Kit (Stratagene, La Jolla, CA). The mutant K11R was generated using primers #837 and #838. K15R was generated using primers #839 and #840. K19R was generated using primers #841 and #842. The final construct (pRM8836) was sequenced to confirm the absence of additional mutations. The sequences of these primers are given in the Supplemental Material.

PAC1-his6. An integration vector for Pac1p was constructed with a his6 tag fused in-frame at its 3′ prime end. A PCR fragment starting at *PAC1* bp699 was synthesized by PCR with *Xho*I and *Bam*HI restriction sites at its termini. This was ligated into the corresponding sites of the vector, pRM2194. This created plasmid pRM9232, which was sequenced to confirm the intended sequence. For integration by one-step gene tagging, the plasmid was linearized with *Cla*I, and transformants were selected on SC media lacking histidine.

REFERENCES

Beach DL, Thibodeaux J, Maddox P, Yeh E, Bloom K (2000). The role of the proteins Kar9 and Myo2 in orienting the mitotic spindle of budding yeast. Curr Biol 10, 1497–1506.

Bekes M, Prudden J, Srikumar T, Raught B, Boddy MN, Salvesen GS (2011). The dynamics and mechanism of SUMO chain deconjugation by SUMO-specific proteases. J Biol Chem 286, 10238–10247.

Bencsath KP, Podgorski MS, Pagala VR, Slaughter CA, Schulman BA (2002). Identification of a multifunctional binding site on Ubc9p required for Smt3p conjugation. J Biol Chem 277, 47938–47945.

Bergman ZJ, Xia X, Amaro IA, Huffaker TC (2012). Constitutive dynein activity in She1 mutants reveals differences in microtubule attachment at the yeast spindle pole body. Mol Biol Cell 23, 2319–2326.

Berlin V, Styles CA, Fink GR (1990). BIK1, a protein required for microtubule function during mating and mitosis in *Saccharomyces cerevisiae*, colocalizes with tubulin. J Cell Biol 111, 2573–2586.

Biggins S, Bhalla N, Chang A, Smith DL, Murrary AW (2001). Genes involved in sister chromatid separation and segregation in the budding yeast *Saccharomyces cerevisiae*. Genetics 159, 453–470.

Blake-Hodek KA, Cassimeris L, Huffaker TC (2010). Regulation of microtubule dynamics by Bim1 and Bik1, the budding yeast members of the EB1 and CLIP-170 families of plus-end tracking proteins. Mol Biol Cell 21, 2013–2023.

Bylebyl GR, Belichenko I, Johnson ES (2003). The SUMO isopeptidase Ulp2 prevents accumulation of SUMO chains in yeast. J Biol Chem 278, 44113–44120.

Carminati JL, Stearns T (1997). Microtubules orient the mitotic spindle in yeast through dynein-dependent interactions with the cell cortex. J Cell Biol 138, 629–641.

Carvalho P, Gupta MLJ, Hoyt MA, Pellman D (2004). Cell cycle control of kinesin-mediated transport of Bik1(CLIP-170) regulates microtubule stability and dynein activation. Dev Cell 6, 815–829.

Caudron F, Andrieux A, Job D, Boscheron C (2008). A new role for kinesin-directed transport of Bik1p (CLIP-170) in *Saccharomyces cerevisiae*. J Cell Sci 121, 1506–1513.

Choi JH, Adames NR, Chan TF, Zeng C, Cooper JA, Zheng XFS (2000). TOR signaling regulates microtubule structure and function. Curr Biol 10, 861–864.

Choi JH, Bertram PG, Drenan R, Carvalho J, Zhou HH, Zheng XFS (2002). The FKBP12-rapamycin-associated protein (FRAP) is a CLIP-170 kinase. EMBO Rep 3, 988–994.

Dasso M (2008). Emerging roles of the SUMO pathway in mitosis. Cell Division 3, 5.

Dorval V, Fraser PE (2006). Small ubiquitin-like modifier (SUMO) modification of natively unfolded proteins tau and alpha-synuclein. J Biol Chem 281, 9919–9924.

Duan X, Holmes WB, Ye H (2011). Interaction mapping between *Saccharomyces cerevisiae* Smc5 and SUMO E3 ligase Mms21. Biochemistry 50, 10182–10188.

Dujardin DL, Barnhart LE, Stehman SA, Gomes ER, Gundersen GG, Vallee RB (2003). A role for cytoplasmic dynein and LIS1 in directed cell movement. J Cell Biol 163, 1205–1211.

Elmore ZC, Donaher M, Matson BC, Murphy H, Westerbeck JW, Kerscher O (2011). SUMO-dependent substrate targeting of the SUMO protease Ulp1. BMC Biol 9, 74.

Farkasovsky M, Küntzel H (2001). Cortical Num1p interacts with the dynein intermediate chain Pac11p and cytoplasmic microtubules in budding yeast. J Cell Biol 152, 251–262.

Faulkner NE, Dujardin DL, Tai C-Y, Vaughan KT, O'Connell CB, Wang YL, Vallee RB (2000). A role for the lissencephaly gene *LIS1* in mitosis and cytoplasmic dynein function. Nat Cell Biol 2, 784–791.

Finley, Bartel DB, Varshavsky A (1989). The tails of ubiquitin precursors are ribosomal proteins whose fusion to ubiquitin facilitates ribosome biogenesis. Nature 338, 394–401.

Fleming JA, Lightcap ES, Sadis S, Thoroddsen V, Bulawa CE, Blackman RK (2002). Complementary whole-genome technologies reveal the cellular response to proteasome inhibition by PS-341. Proc Natl Acad Sci USA 99, 1461–1466.

Gareau JR, Lima CD (2010). The SUMO pathway: emerging mechanisms that shape specificity, conjugation and recognition. Nat Rev Mol Cell Biol 11, 861–871.

Han G, Liu B, Zhang J, Zuo W, Morris NR, Xiang X (2001). The *Aspergillus* cytoplasmic dynein heavy chain and NUDF localize to microtubule ends and affect microtubule dynamics. Curr Biol 11, 719–724.

He X, Rines DR, Espelin CW, Sorger PK (2001). Molecular analysis of kinetochore-microtubule attachment in budding yeast. Cell 106, 195–206.

Heideker J, Prudden J, Perry JJP, Tainer JA, Boddy MN (2011). SUMO-targeted ubiquitin ligase, Rad60, and Nse2 SUMO ligase suppress spontaneous Top1-mediated DNA damage and genome instability. PLoS Genet 7, e10001320.

Heil-Chapdelaine RA, Oberle JR, Cooper JA (2000). The cortical protein Num1p is essential for dynein-dependent interactions of microtubules with the cortex. J Cell Biol 151, 1337–1344.

Huang J, Roberts AJ, Leschziner AE, Reck-Peterson SL (2012). Lis1 acts as a "clutch" between the ATPase and microtubule binding domains of the dynein motor. Cell 150, 975–986.

Hwang E, Kusch EJ, Barral Y, Huffaker TC (2003). Spindle orientation in *Saccharomyces cerevisiae* depends on the transport of microtubule ends along polarized actin cables. J Cell Biol 161, 483–488.

James P, Halladay J, Craig EA (1996). Genomic libraries and a host strain designed for highly efficient two-hybrid selection in yeast. Genetics 144, 1425–1436.

Johnson ES, Blobel G (1997). Ubc9p is the conjugating enzyme for the ubiquitin-like protein Smt3p. J Biol Chem 272, 26799–26802.

Johnson ES, Gupta AA (2001). An E3-like factor that promotes SUMO conjugation to the yeast septins. Cell 106, 735–744.

Kahana JA, Schnapp BJ, Silver PA (1995). Kinetics of spindle pole body separation in budding yeast. Proc Natl Acad Sci USA 92, 9707–9711.

Kolli N, Mikolajczyk J, Drag M, Mukhopadhyay D, Moffatt N, Dasso M, Salvesen G, Wilkinson KD (2010). Distribution and paralogue specificity of mammalian deSUMOylating enzymes. Biochem J 430, 335–344.

Lam C, Vergnolle MA, Thorpe L, Woodman PG, Allan VJ (2010). Functional interplay between LIS1, NDE1 and NDEL1 in dynein-dependent organelle positioning. J Cell Sci 123, 202–212.

Lee L, Tirnauer JS, Li J, Schuyler SC, Liu JY, Pellman D (2000). Positioning of the mitotic spindle by a cortical-microtubule capture mechanism. Science 287, 2260–2262.

Lee WL, Kaiser MA, Cooper JA (2005). The offloading model for dynein function: differential function of motor subunits. J Cell Biol 168, 201–207.

Lee WL, Oberle JR, Cooper JA (2003). The role of the lissencephaly protein Pac1 during nuclear migration in budding yeast. J Cell Biol 160, 355–364.

Leisner C, Kammerer D, Denoth A, Britschi M, Barral Y, Liakopoulos D (2008). Regulation of mitotic spindle asymmetry by SUMO and the spindle-assembly checkpoint in yeast. Curr Biol 18, 1249–1255.

Li J, Lee WL, Cooper JA (2005). NudEL targets dynein to microtubule ends through LIS1. Nat Cell Biol 7, 686–690.

Li SJ, Hochstrasser M (1999). A new protease required for cell-cycle progression in yeast. Nature 398, 246–251.

Li SJ, Hochstrasser M (2000). The yeast *ULP2(SMT4)* gene encodes a novel protease specific for the ubiquitin-like Smt3 protein. Mol Cell Biol 20, 2367–2377.

Liakopoulos D, Kusch J, Grava S, Vogel J, Barral Y (2003). Asymmetric loading of Kar9 onto spindle poles and microtubules ensures proper spindle alignment. Cell 112, 561–574.

Lin H, de Carvalho P, Kho D, Tai CY, Pierre P, Fink GR, Pellman D (2001). Polyploids require Bik1 for kinetochore-microtubule attachment. J Cell Biol 155, 1173–1184.

Maekawa H, Schiebel E (2004). Cdk1-Clb4 controls the interaction of astral microtubule plus ends with subdomains of the daughter cell cortex. Genes Dev 18, 1709–1724.

Markus SM, Plevock KM, St. Germain BJ, Punch JJ, Meaden CW, Lee WL (2011). Quantitative analysis of Pac1/Lis1-mediated dynein targeting: Implications for regulation of dynein activity in budding yeast. Cytoskeleton 68, 157–174.

McKenney RJ, Vershinin J, Kunwar A, Vallee RB, Gross SP (2010). Lis1 and NudE induce a persistent dynein force-producing state. Cell 141, 304–314.

McKenney RJ, Weil SJ, Scherer J, Vallee RB (2011). Mutually exclusive cytoplasmic dynein regulation by NudE-Lis1 and dynactin. J Biol Chem 286, 39615–39622.

McMillan JN, Tatchell K (1994). The *JNM1* gene in the yeast *Saccharomyces cerevisiae* is required for nuclear migration and spindle orientation during the mitotic cell cycle. J Cell Biol 125, 143–158.

Meednu N, Hoops H, D'Silva S, Pogorzala L, Wood S, Farkas D, Sorrentino M, Sia E, Meluh P, Miller RK (2008). The spindle positioning protein Kar9p interacts with the sumoylation machinery in *Saccharomyces cerevisiae*. Genetics 180, 2033–2055.

Miller RK, Cheng S-C, Rose MD (2000). Bim1p/Yeb1p mediates the Kar9p-dependent cortical attachment of cytoplasmic microtubules. Mol Biol Cell 11, 2949–2959.

Miller RK, Heller KK, Frisen L, Wallack DL, Loayza D, Gammie AE, Rose MD (1998). The kinesin-related proteins, Kip2p and Kip3p, function differently in nuclear migration in yeast. Mol Biol Cell 9, 2051–2068.

Miller RK, Matheos D, Rose MD (1999). The cortical localization of the microtubule orientation protein, Kar9p, is dependent upon actin and proteins required for polarization. J Cell Biol 144, 963–975.

Miller RK, Moore JK, D'Silva S, Goodson HV (2006). The CLIP-170 orthologue Bik1p and positioning the mitotic spindle in yeast. Curr Topics Dev Biol 49–87.

Miller RK, Rose MD (1998). Kar9p is a novel cortical protein required for cytoplasmic microtubule orientation in yeast. J Cell Biol 140, 377–390.

Molk JN, Salmon ED, Bloom K (2006). Nuclear congression is driven by cytoplasmic microtubule plus end interactions in *S. cerevisiae*. J Cell Biol 172, 27–39.

Montpetit B, Hazbun TR, Fields S, Hieter P (2006). Sumoylation of the budding yeast kinetochore protein Ndc10 is required for Ndc10 spindle localization and regulation of anaphase spindle elongation. J Cell Biol 174, 653–663.

Moore JK, D'Silva S, Miller RK (2006). The CLIP-170 homologue Bik1p promotes the phosphorylation and asymmetric localization of Kar9p. Mol Biol Cell 17, 178–191.

Moore JK, Li J, Cooper JA (2008). Dynactin function in mitotic spindle positioning. Traffic 9, 510–527.

Moore JK, Miller RK (2007). The cyclin-dependent kinase Cdc28p regulates multiple aspects of Kar9p function in yeast. Mol Biol Cell 18, 1187–1202.

Mukhopadhyay D, Dasso M (2007). Modification in reverse: the SUMO proteases. Trends Biochem Sci 32, 286–295.

Mullen JR, Chem CF, Brill SJ (2010). Wss1 is a SUMO-dependent isopeptidase that interacts genetically with the Slx5-Slx8 SUMO-targeted ubiquitin ligase. Mol Cell Biol 30, 3737–3748.

Praefcke GJ, Hofmann K, Dohmen RJ (2012). SUMO playing tag with ubiquitin. Trends Biochem Sci 37, 23–31.

Reindle A, Belichenko I, Bylebyl GR, Chen XL, Gandhi N, Johnson ES (2006). Multiple domains in Siz SUMO ligases contribute to substrate selectivity. J Cell Sci 119, 4749–4757.

Reiner O, Sapoznik S, Sapir T (2006). Lissencephaly 1 linking to multiple diseases: mental retardation, neurodegeneration, schizophrenia, male sterility, and more. Neuromolecular Med 8, 547–565.

Sapir T, Elbaum M, Reiner O (1997). Reduction of microtubule catastrophe events by LIS1, platelet-activating factor acetylhydrolase subunit. EMBO J 16, 6977–6984.

Sarge KD, Park-Sarge OK (2011). SUMO and its role in human diseases. Int Rev Cell Mol Biol 288, 167–183.

Schwartz K, Richards K, Botstein D (1997). BIM1 encodes a microtubule-binding protein in yeast. Mol Biol Cell 8, 2677–2691.

Sheeman B, Carvalho P, Sagot I, Geiser J, Kho D, Hoyt MA, Pellman D (2003). Determinants of S. cerevisiae dynein localization and activation: implications for the mechanism of spindle positioning. Curr Biol 13, 364–372.

Shu T, Ayala R, Nguyen MD, Xie Z, Gleeson JG, Tsai LH (2004). Ndel1 operates in a common pathway with LIS1 and cytoplasmic dynein to regulate cortical neuronal positioning. Neuron 44, 263–277.

Sikorski RS, Hieter P (1989). A system of shuttle vectors and yeast host strains designed for efficient manipulation of DNA in Saccharomyces cerevisiae. Genetics 122, 19–27.

Stephan AK, Kliszczak M, Morrison CG (2011). The Nse/Mms21 SUMO ligase of the Smc5/6 complex in the maintenance of genome stability. FEBS Lett 585, 2907–2913.

Su D, Hochstrasser M (2010). A WLM protein with SUMO-directed protease activity. Mol Cell Biol 30, 3734–3736.

Su X, Qiu W, Gupta Jr ML, Pereira-Leal JB, Reck-Peterson SL, Pellman D (2011). Mechanisms underlying the dual-mode regulation of microtubule dynamics by Kip3/kinesin-8. Mol Cell 43, 751–763.

Sumigray KD, Chen H, Lechler T (2011). Lis1 is essential for cortical microtubule organization and desmosome stability in the epidermis. J Cell Biol 194, 631–642.

Sun H, Leverson JD, Hunter T (2007). Conserved function of RNF4 family proteins in eukaryotes: targeting a ubiquitin ligase to SUMOylated proteins. EMBO J 26, 4102–4112.

Takahashi K, Ishida M, Komano H, Takahashi H (2008). SUMO-1 immunoreactivity co-localizes with phospho-Tau in APP transgenic mice but not in mutant Tau transgenic mice. Neurosci Lett 441, 90–93.

Tanaka T, Serneo FF, Higgins C, Gambello MJ, Wynshaw-Boris A, Gleeson JG (2004). Lis1 and doublecortin function with dynein to mediate coupling of the nucleus to the centrosome in neuronal migration. J Cell Biol 165, 709–721.

Torisawa T, Nakayama A, Furuta K, Yamada M, Hirotsune S, Toyoshima YY (2011). Functional dissection of LIS1 and NDEL1 towards understanding the molecular mechanisms of cytoplasmic dynein regulation. J Biol Chem 286, 1959–1965.

Tsai JW, Bremner KH, Vallee RB (2007). Dual subcellular roles for LIS1 and dynein in radial neuronal migration in live brain tissue. Nat Neurosci 10, 970–979.

Tsai JW, Chen Y, Kriegstein AR, Vallee RB (2005). LIS1 RNA interference blocks neural stem cell division, morphogenesis, and motility at multiple stages. J Cell Biol 170, 935–945.

Tsai JW, Lian WN, Kemal S, Kriegstein AR, Vallee RB (2010). Kinesin 3 and cytoplasmic dynein mediate interkinetic nuclear migration in neural stem cells. Nat Neurosci 13, 1463–1471.

Uzunova K et al. (2007). Ubiquitin-dependent proteolytic control of SUMO conjugates. J Biol Chem 282, 34167–34175.

Westermann S, Drubin DG, Barnes G (2007). Structures and functions of yeast kinetochore complexes. Annu Rev Biochem 76, 563–591.

Wolyniak MJ, Blake-Hodek K, Kosco K, Hwang E, You L, Huffaker TC (2006). The regulation of microtubule dynamics in Saccharomyces cerevisiae by three interacting plus end tracking proteins. Mol Biol Cell 17, 2789–2798.

Woodruff JB, Drubin DG, Barnes G (2009). Dynein-driven mitotic spindle positioning restricted to anaphase by She1p inhibition of dynactin recruitment. Mol Biol Cell 20, 3003–3011.

Wong J et al. (2007). A protein interaction map of the mitotic spindle. Mol Biol Cell 18, 3800–3809.

Xie Y, Kerscher O, Kroetz MB, McConchies HF, Sung P, Hochstrasser M (2007). The yeast Hex3-Slx8 heterodimer is a ubiquitin ligase stimulated by substrate sumoylation. J Biol Chem 282, 34176–34184.

Yeh E, Skibbens RV, Cheng JW, Salmon ED, Bloom K (1995). Spindle dynamics and cell cycle regulation of dynein in the budding yeast, Saccharomyces cerevisiae. J Cell Biol 130, 687–700.

Yeh ET (2009). SUMOylation and De-SUMOylation: wrestling with life's processes. J Biol Chem 284, 8223–8227.

Yi JY, Ori-McKenny KM, McKenney RJ, Vershinin M, Gross SP, Vallee RB (2011). High-resolution imaging reveals indirect coordination of opposite motors and a role for LIS1 in high-load axonal transport. J Cell Biol 195, 193–201.

Yin HDP, Huffaker TC, Bretscher A (2000). Myosin V orientates the mitotic spindle in yeast. Nature 406, 1013–1015.

Zhang J, Zhuang L, Lee Y, Abenza JF, Penalva MA, Xiang X (2010). The microtubule plus-end localization of Aspergillus dynein is important for dynein-early-endosome interaction but not for dynein ATPase activation. J Cell Sci 123, 3596–3604.

Zhang XD, Goeres J, Zhang H, Yen TJ, Porter AC, Matunis MJ (2008). SUMO-2/3 modification and binding regulate the association of CENP-E with kinetochores and progression through mitosis. Mol Cell 29, 729–741.

Zhou W, Ryan JJ, Zhou H (2004). Global analyses of sumoylated proteins in Saccharomyces cerevisiae: Induction of protein sumoylation by cellular stresses. J Biol Chem 279, 32262–32268.